

# PHYSICAL ORGANIC METHODS IN CAROTENOID RESEARCH

U. SCHWIETER, G. ENGLERT, N. RIGASSI AND W. VETTER

*Research Department, F. Hoffmann-La Roche & Co. Ltd., Basle, Switzerland*

## ABSTRACT

The ever increasing importance of physical methods in the elucidation of the structure and configuration of carotenoids is reviewed. The use of solvent partition, chromatography, X-ray crystallography, infra-red spectroscopy and optical rotary dispersion are briefly discussed. Special emphasis is given to the application of absorption spectroscopy and to 220 MHz proton magnetic resonance spectroscopy of carotenoids.

Mass spectroscopic studies of the characteristic fragmentation of the carotenes, and a possible mechanism for the fragmentation of the polyene chain, are discussed in detail.

\* \* \*

Physical organic methods have exerted an extremely stimulating influence on carotenoid research. Prior to the routine application of these methods polyene chemistry has been very troublesome in comparison with today's efforts in this field. About twenty years ago, the main tool for routine analysis of, for instance, chromatographic fractions was the Carr-Price reaction: in chloroform solution an unsaturated compound when mixed with antimony trichloride, trichloroacetic or sulphuric acid gives a very pronounced bathochromic shift. Vitamin A is the most prominent example because here the Carr-Price reaction is still in use as an analytical method. In the colourless chloroform solution a transient deep blue colour arises. The draw-back of the Carr-Price reaction was that, lacking spectrophotometric apparatus, one had to guess the colour of an intermediate polyene and one usually guessed wrong. It might even be said, that if the intermediates did not crystallize and thus could not be sent for C.H.-analysis, the proof of their structure was more or less the identity of the final product with the known natural material. This caused time consuming arduous syntheses but, in retrospect, it also increases our admiration for these early efforts.

A possible mechanism for the reaction has been discussed: the mesomeric allylic carbonium ions shown in *Figure 1* for vitamin A and anhydro-vitamin A are considered responsible for the bathochromic shift<sup>1</sup>.

Since the protonation of lycopene has been studied<sup>2</sup>, one might argue that, in analogy, the colour reaction of the carotenes can be explained as shown in *Figure 2*.

The approximate position of the absorption maximum of the Carr-Price reaction can be calculated:

$$\lambda_{\max} = 300.5 + 65.5 \times n$$

where  $n$  represents the number of effective double bonds (i.e. 5 for vitamin A, 10 for  $\beta$ -carotene)<sup>3</sup>. This equation has been found to give good values

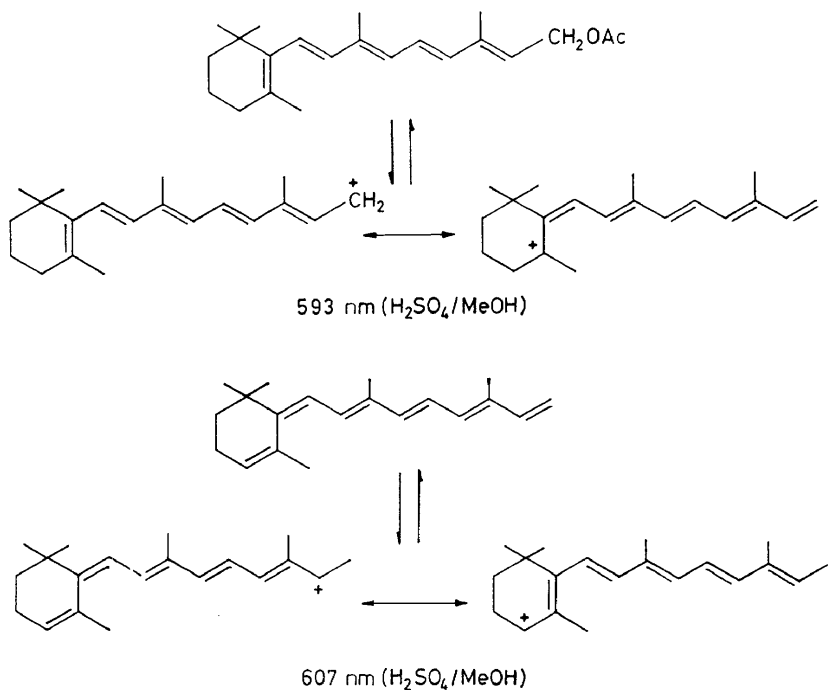


Figure 1. Postulated mechanism for the Carr-Price reaction of vitamin A and anhydro-vitamin A.

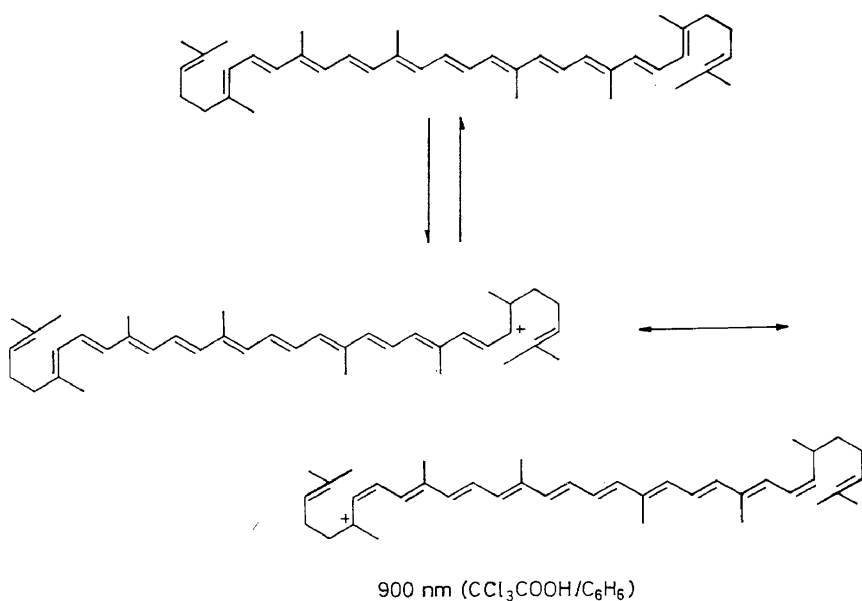
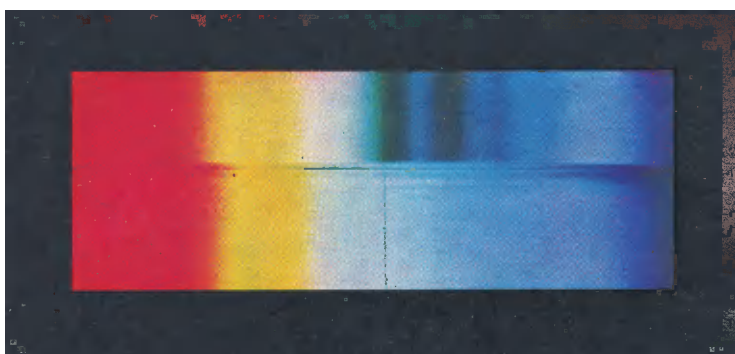


Figure 2. Carr-Price reaction of lycopene.



*Figure 3.* Ultraviolet and visible light absorption spectrum of lycopene (in ethanol) taken with a Zeiss grating spectroscope.

for the reaction in 80 per cent sulphuric acid. The equation also seems to give satisfactory results for the reaction in other solvents.

With the availability of new physical methods the pace of synthesis began to quicken; new methods for the synthesis of polyenes could be developed<sup>4</sup>. New structures of minor or complicated carotenoids could be elucidated. With the ever increasing number of synthetic and naturally occurring materials available for comparison, the physical organic methods led in turn to very valuable empirical rules.

Because of the complexity of the methods, a review of such 'rules of thumb' has to be selective.

*Partition* into an epiphasic, unpolar fraction and a hypophasic, polar fraction was and still is a helpful tool for a rough separation of a carotenoid mixture. However, in order to be effective this method has to be performed under standard conditions. Today, chromatography is a more reliable method and therefore partition has lost most of its value.

*Column, paper and thin layer chromatography*, although extremely valuable for the identification and purification of polyenes, are never exactly reproducible. They depend in most cases upon the co-chromatography of a closely related or identical sample. An important method for the proof of identity of small samples with known carotenoids is the co-chromatography of the iodine isomerized equilibrium mixtures. However, all existing evidence suggests that it is quite unlikely that we will ever be able to calculate *a priori*  $R_f$  values. Trends, however, can often be seen. For instance, compounds with an  $\alpha$ -end group usually have larger  $R_f$  values than the corresponding  $\beta$ -compounds, which in turn run faster than the  $\gamma$ -, or pseudoanalogues. Accordingly  $\epsilon$ -carotene with two  $\alpha$ -end groups has the largest  $R_f$  value, followed by the  $\alpha,\beta$ -( $\alpha$ -carotene);  $\beta,\beta$ -( $\beta$ -carotene),  $\alpha,\gamma$ -( $\delta$ -carotene);  $\beta,\gamma$ -( $\gamma$ -carotene) and  $\gamma,\gamma$ -analogues (lycopene)<sup>19c</sup>.

## ABSORPTION SPECTROSCOPY

Absorption spectroscopy has been used for the characterization of carotenoids for some forty years. Many different types of spectroscopes and photometers were used in those days, which caused conflicting results with regard to the position of the absorption maxima and their extinction coefficients<sup>5</sup>. As an example the spectrum of lycopene in ethanol solution taken with a Zeiss grating spectroscope is shown in *Figure 3*. In the upper half of the picture a number of dark absorption bands are seen in comparison with the continuous spectrum of the solvent below. The position of the absorption bands is measured by moving the cross hairs over the spectrum. Here they are centred at the 503 nm band. A quantitative analysis can only be obtained by measuring the intensity of blackening of a photographic plate.

The autocatalytic influence of physico-organic methods on carotenoid research began in the late forties with the introduction of fast scanning spectrophotometers, which allowed a rapid and accurate quantitative analysis.

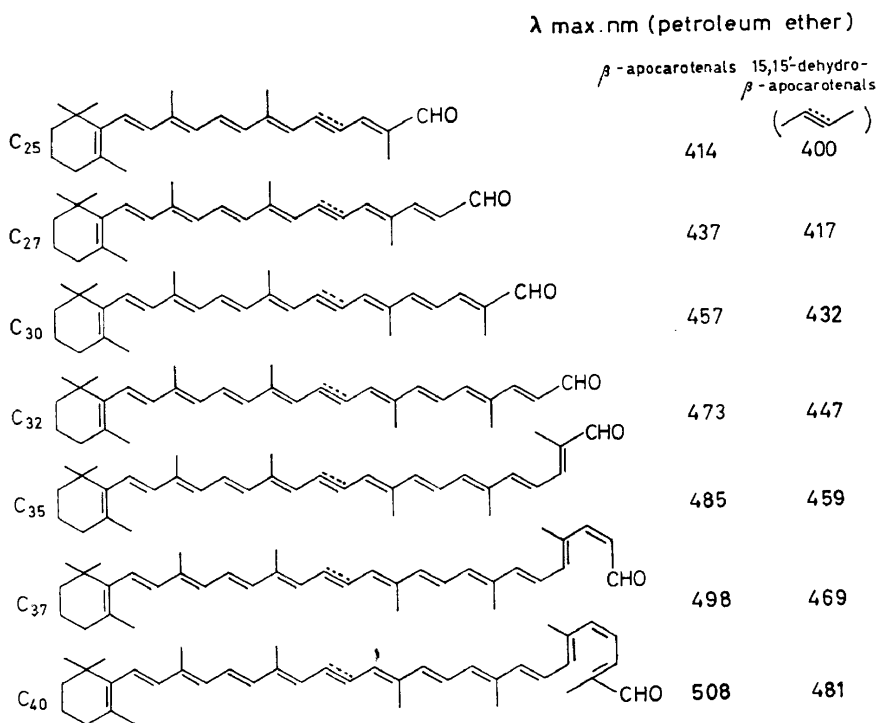
Spectra of polyenes show, in addition to the main absorption band with its vibrational fine structure, minor peaks with or without fine structure. Under standard conditions the shape of the spectrum is determined by the

number of double bonds, the substituents, *cis-trans* isomerism and by the solvent. *Table 1* summarizes a first approximation of these influences.

*Table 1.* Influences of substituents and solvents on the main absorption maximum of carotenoids

double bond	aliphatic	+7 to +35 nm
double bond	ring	+5 to +9 nm
first carbonyl	aliphatic	+28 nm
second carbonyl	aliphatic	+1 to +7 nm
first carbonyl	ring	+7 nm
second carbonyl	ring	+5 to +9 nm
first carbonyl	ring retro	+9 nm
second carbonyl	ring retro	+5 nm
first and second	5,6-epoxide	-8 nm
first and second	5,8-epoxide	-20 nm
trans→cis		-4 nm
normal→retro		-10 nm
solvent effect:	ethanol, hexane, petrol. ether:	small effect
	benzene, chloroform	+15 nm
	carbon disulphide	+35 nm

One can see that double bonds have a varying contribution to the position of the main absorption band. This is exemplified in *Figure 4* for the apocarotenal series. The bathochromic shift for one additional double bond is



*Figure 4.* Visible light absorption maxima of β-apocarotenals and their 15,15-dehydro analogues (in petroleum ether).

23 nm for the first two compounds in contrast to only 10 nm for the last two members of this series. The 15,15'-dehydro analogues show the same decreasing contribution for each additional double bond. In the beginning of the series the difference is 17 nm and at the end 10 nm. The conjugated triple bond exerts a marked hypsochromic shift, the degree of which is, however, dependent upon its position in the conjugated chain. The hypsochromic shift is 14 nm when a triple bond is introduced at the  $\gamma,\delta$ -position of the  $\beta$ -apo-12'-carotenal ( $C_{25}$ ). However, it is 27 nm when the triple bond is almost at the centre of the conjugated chain as in the torularhodinaldehyde analogues with 40 carbon atoms.

Of the  $C_{40}$ -carotenes lycopene has its absorption maxima at the longest wavelengths. On ring-closure, the terminal conjugated double bond can either remain in conjugation ( $\beta$ -end group) or it is moved out of conjugation ( $\alpha$ -end group). Figures 5-6 indicate the change of the absorption bands for this ring-closure, first with the conjugated double bonds remaining in their position. When ring-closure occurs at one end of the molecule ( $\gamma$ -carotene) a loss of fine structure and a hypsochromic shift as well as a hypochromic effect are observed. This is even more pronounced upon closure of the second ring ( $\beta$ -carotene).

Although one conjugated double bond is lost on  $\alpha$ -ring-closure as seen in

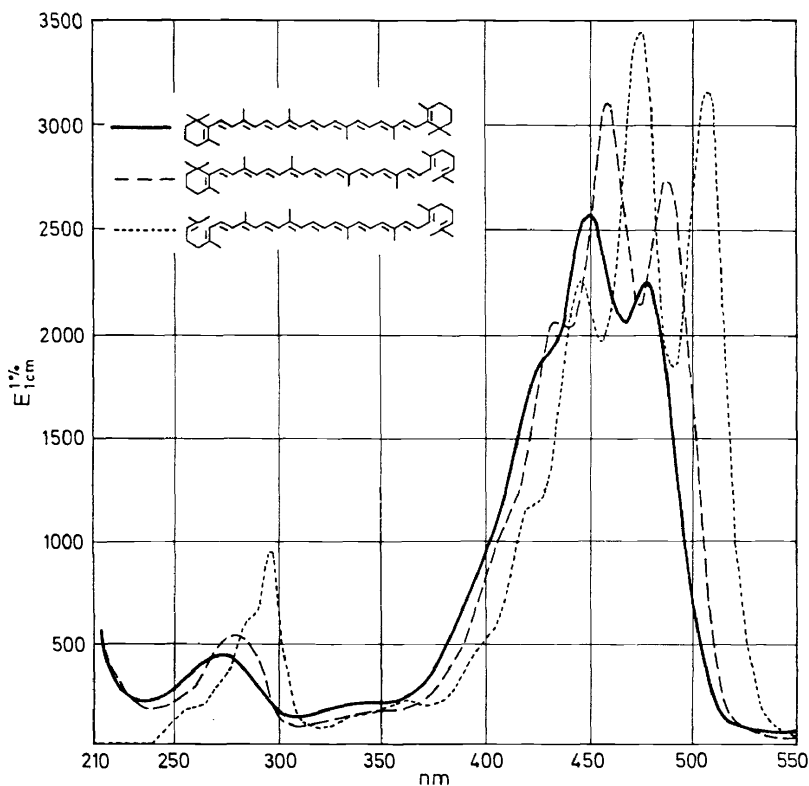


Figure 5. Ultraviolet and visible light absorption spectra of lycopene ( $\cdots$ ),  $\gamma$ -carotene ( $-\cdots-$ ) and  $\beta$ -carotene ( $————$ ) (in petroleum ether).

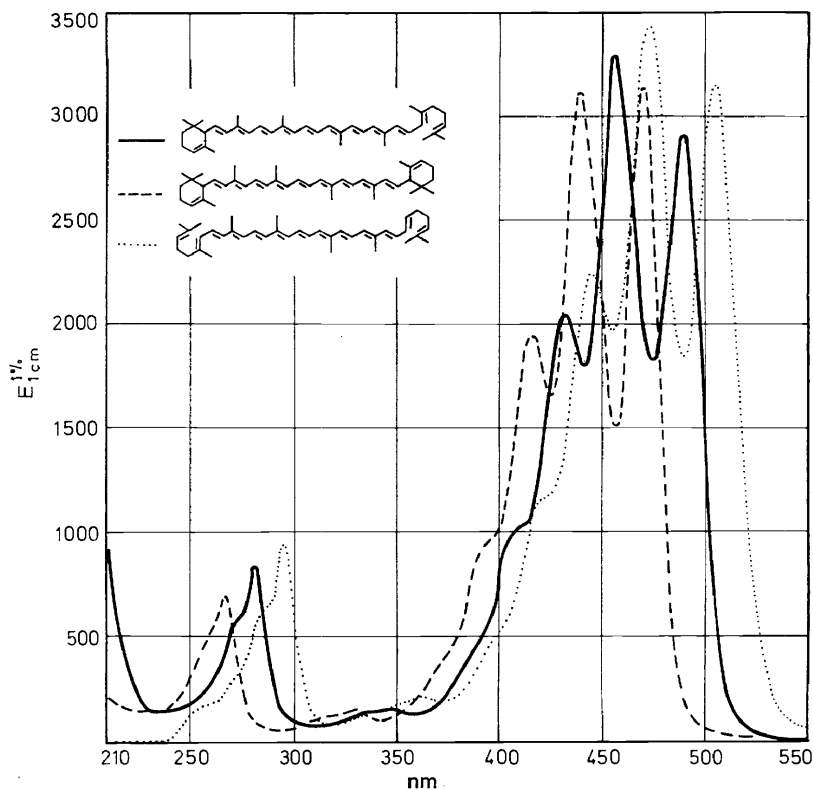


Figure 6. Ultraviolet and visible light absorption spectra of lycopene ( $\cdots$ ),  $\epsilon$ -carotene ( $---$ ) and  $\delta$ -carotene ( $—$ ) (in petroleum ether).

Figure 6, a hypsochromic shift of only 6 nm is observed for each conversion of a  $\beta$ - to an  $\alpha$ -end group. The shift for  $\delta$ -carotene, which has one  $\alpha$ -end group, is 6 nm, while that of  $\epsilon$ -carotene is 13 nm. Compounds with  $\alpha$ -end groups retain the fine structure of the main absorption band and have a much higher extinction coefficient than the  $\beta$ -analogues.

Figure 7 shows the effect of the introduction of a conjugated carbonyl group in the intact carotene molecule. If one carbonyl group is introduced at the 4-position of  $\beta$ -carotene (echinenone), a hypsochromic effect and bathochromic shift are observed with a complete loss of fine structure. The introduction of a second carbonyl-function in the 4'-position (canthaxanthin) causes a small bathochromic displacement of the broad absorption maximum.

The end groups can be removed by a hypothetical oxidation of the 7,8(7',8')-double bonds, giving alcohols, aldehydes or carboxylic acid esters.  $\beta$ -Carotene, for instance, would give  $\beta$ -apo-8'-carotenal( $C_{30}$ ) if one end group were removed, or crocetin dialdehyde upon the loss of both end groups (Figure 8). Each removal causes a hyperchromic effect, with hardly any shift of the main absorption maximum, although the fine structure becomes more and more apparent.

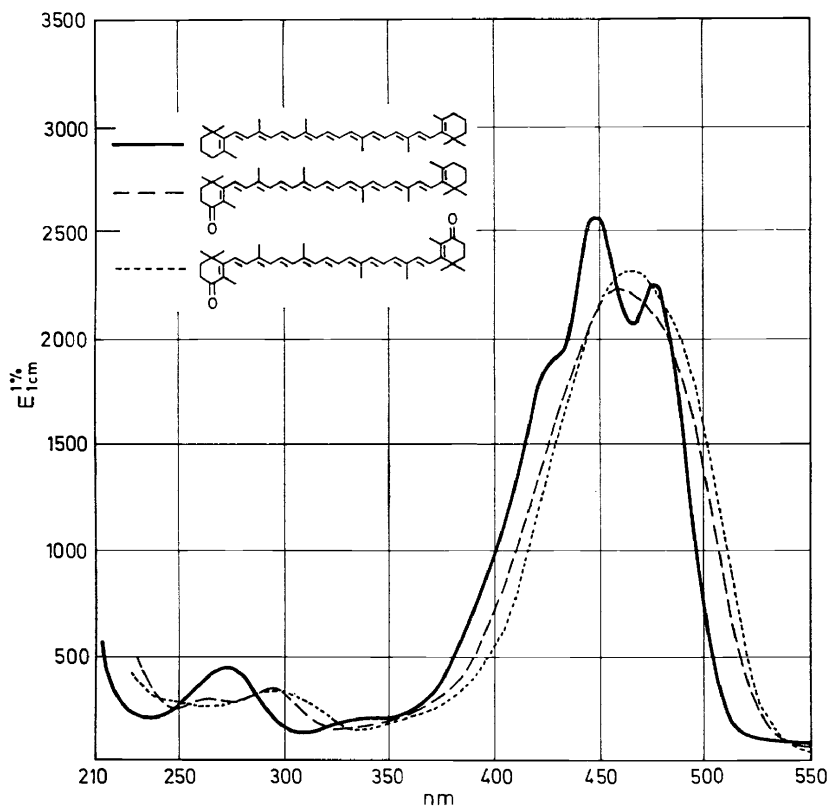


Figure 7. Ultraviolet and visible light absorption spectra of  $\beta$ -carotene (—), echinenone (---) and canthaxanthin (···) (in petroleum ether).



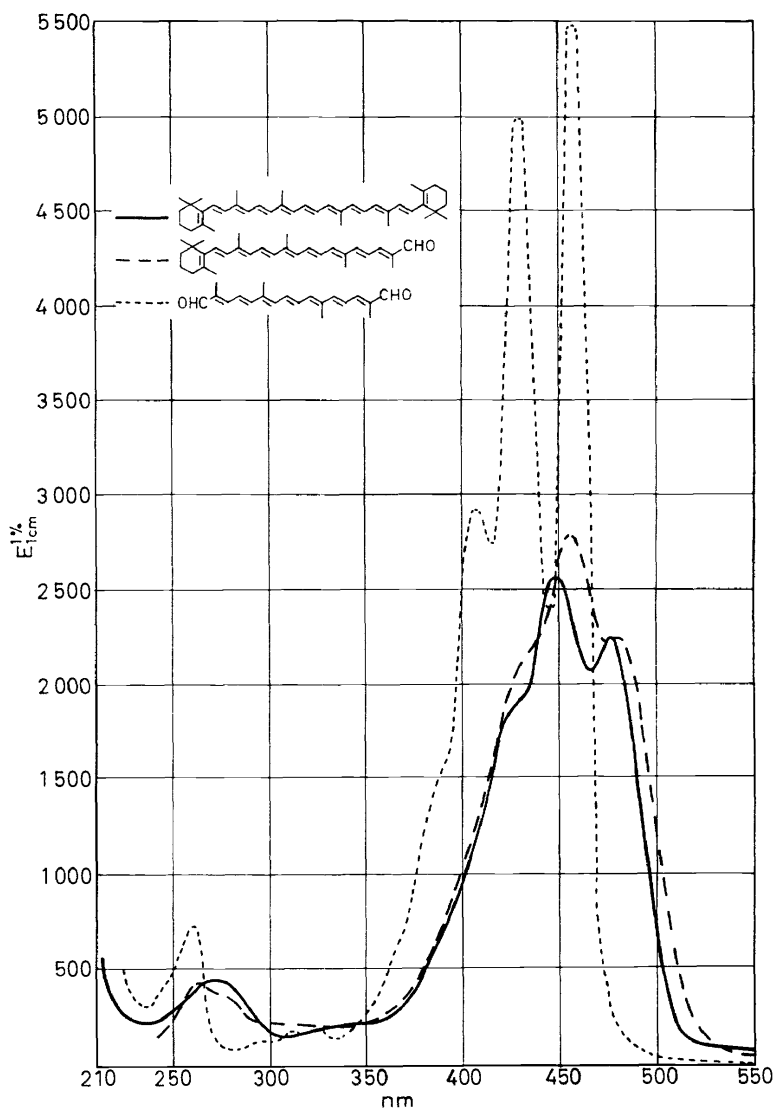
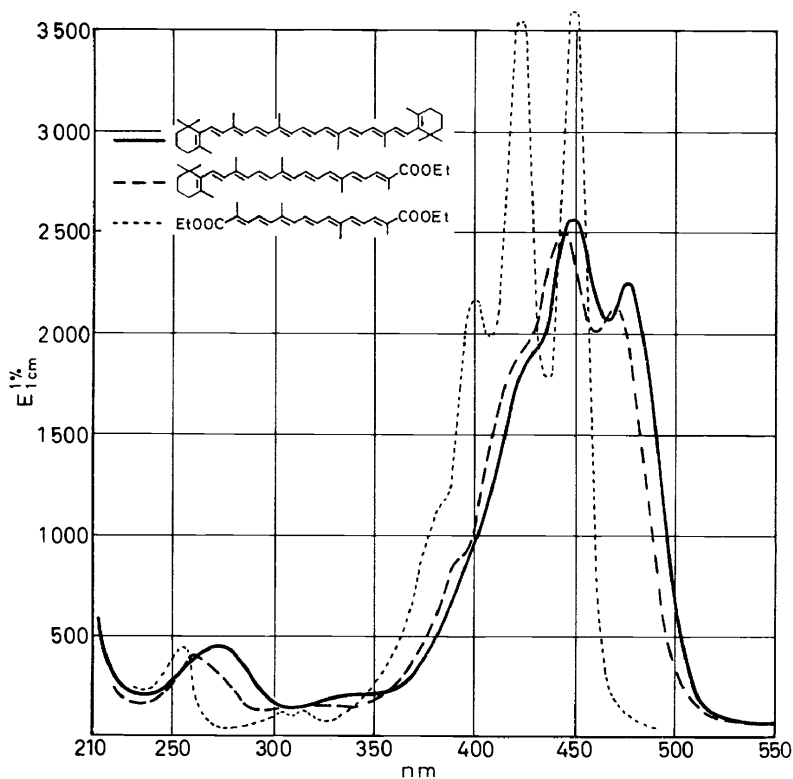


Figure 8. Ultraviolet and visible light absorption spectra of  $\beta$ -carotene (—),  $\beta$ -apo-8'-carotenal( $C_{30}$ ) (---) and crocetin dialdehyde (···) (in petroleum ether).

The ester analogues, i.e.  $\beta$ -apo-8'-carotenoic acid( $C_{30}$ ) ethyl ester and crocetin diethyl ester give the same overall picture: an increase of fine structure and of the extinction coefficient. However, the contribution of an ester group is less than that of a conjugated aldehyde group and results in an overall small hypsochromic shift (*Figure 9*).



*Figure 9.* Ultraviolet and visible light absorption spectra of  $\beta$ -carotene (—), ethyl  $\beta$ -apo-8'-carotenoate( $C_{30}$ ) (---) and crocetin diethyl ester (····) (in petroleum ether).

The corresponding alcohols, i.e.  $\beta$ -apo-8'-carotenol ( $C_{30}$ ) and the  $C_{20}$ -diol show the same trend: increase of fine structure on removal of the  $\beta$ -end groups and the expected hypsochromic shift due to loss of conjugated double bonds (*Figure 10*).

The change from the linear all-*trans* configuration to a two dimensional angular-shaped *cis*-isomer results in the appearance of a subsidiary peak

about 140 nm below the longest absorption maximum of the all-*trans* carotene<sup>6</sup>. In Figure 11 this effect is demonstrated for  $\beta$ -carotene and its central 15,15'-*cis* isomer, the latter showing clearly a lower extinction coefficient and a small hypsochromic shift. The spectrum of  $\beta$ -carotene in ethanol is also shown in this figure, however, the solvent effect is not very pronounced. A solvent effect is seen in Figure 12 for ethyl  $\beta$ -apo-8'-carotenoate.

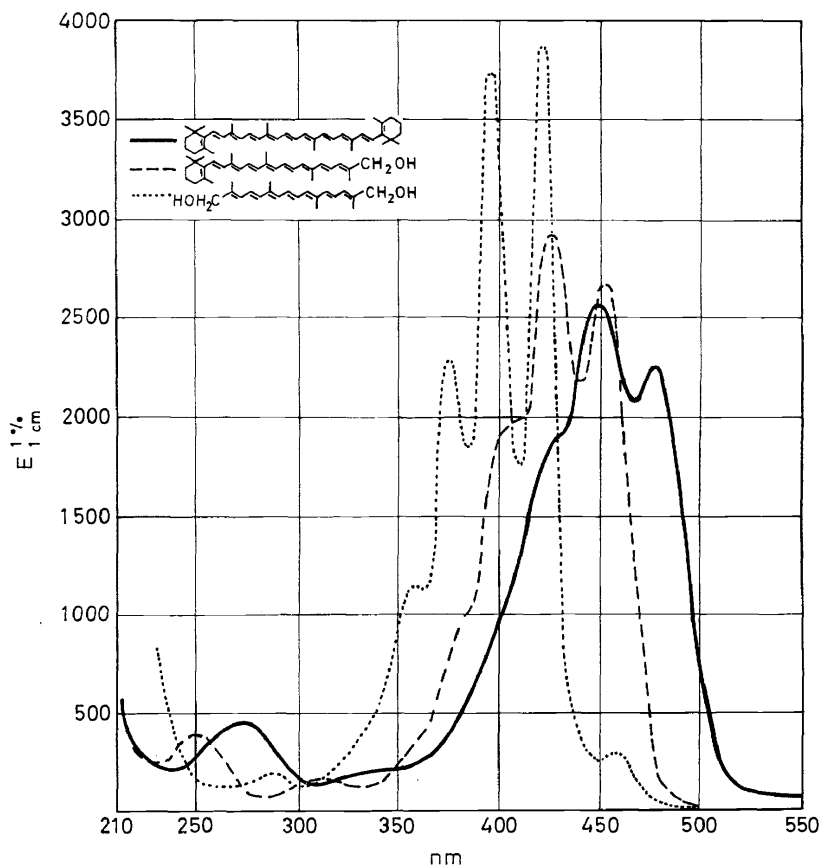


Figure 10. Ultraviolet and visible light absorption spectra of  $\beta$ -carotene (—),  $\beta$ -apo-8'-carotenol ( $C_{30}$ ) (---) and crocetin diol ( $\cdots$ ) (in petroleum ether).

The main absorption band can be calculated according to the general formula given in Table 2. The values of A and B depend upon the solvent and the type of polyene studied. N is determined by the number of conjugated double bonds and their substitution pattern. One conjugated double bond is equivalent to one unit. Subtractions are made for double bonds which are not fully effective, as for instance the bond in the  $\beta$ -ionone ring. The values for several different substituents are given in Table 3.

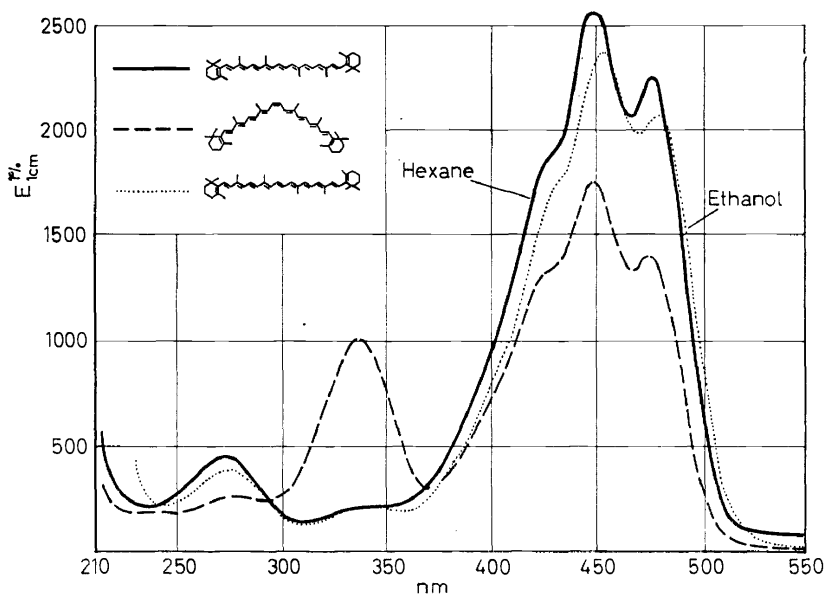


Figure 11. Ultraviolet and visible light absorption spectra of  $\beta$ -carotene (— in hexane, ··· in ethanol) and 15,15'-*cis*- $\beta$ -carotene (--- in hexane).

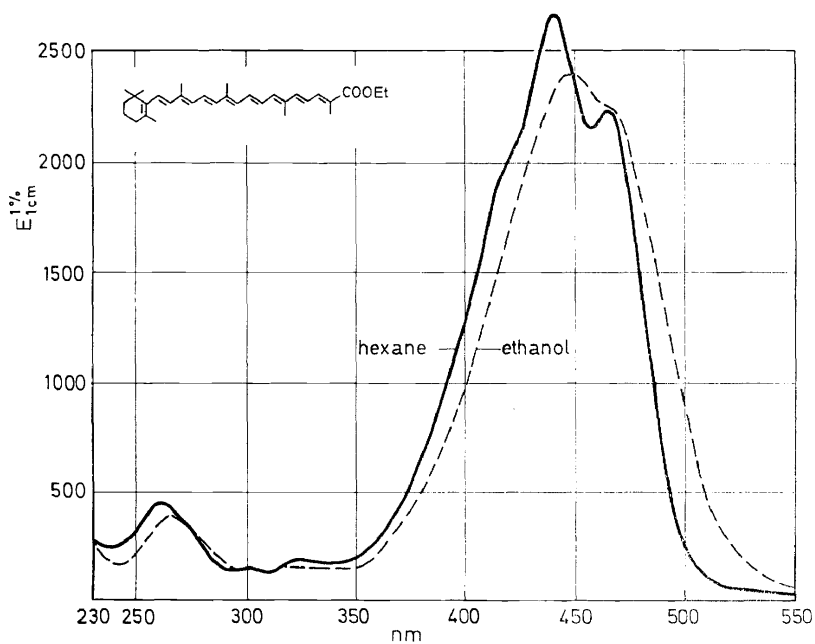


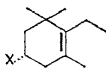
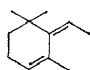
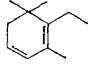
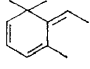
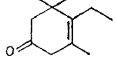
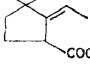
Figure 12. Ultraviolet and visible light absorption spectra of ethyl  $\beta$ -apo-8'-carotenoate ( $C_{30}$ ) in hexane (—) and ethanol (---).

Table 2. Formulae for the calculation of the main absorption maximum of polyenes according to Hirayama<sup>7</sup>.

$(\lambda_{\max})^2 = (A - B \times 0.920^N) \times 10^4 \text{ nm}^2$		<i>A</i>	<i>B</i>
aliphatic polyenes	(hexane)	36.62	38.72
	(ethanol)	36.98	39.10
	(chloroform)	38.60	40.72
$\alpha$ -carbonyl polyenes	(petroleum ether)	39.78	39.33
$\alpha, \omega$ -dicarbonyl polyenes	(petroleum ether)	37.69	34.67

Table 3. Increments (*n*) for substituents and conjugated double bonds for the calculation of the main absorption maximum of polyenes according to Hirayama<sup>7</sup>.

$$(n_1 + n_2 + n_3 \dots \text{etc.} = \Lambda')$$

conjugated double bond	+1.00
alkyl, $\alpha$ -acyloxyalkyl, $\alpha$ -alkoxyalkyl in $\alpha$ or $\omega$	+0.13
second <i>R</i> in $\alpha$ or $\omega$	+0.17
substituent in position other than $\alpha$ or $\omega$	+0.09
$\alpha$ -hydroxyalkyl in $\alpha$ or $\omega$	+0.15
$\alpha$ -hydroxyalkyl in other positions than $\alpha$ or $\omega$	+0.11
$\alpha, \beta$ -epoxyalkyl	+0.18
furanoid oxide	+0.02
exocyclic ethylene linkage	+0.07
endocyclic ethylene linkage	+0.04
1,2-dihydrobenzene structure	+0.83
carboxylic acid	+0.30
	-0.81
	-0.57
	-1.04
	-0.20
	-0.90
	-0.39

The formulae do not, however, always give satisfactory results. Interestingly, they do allow the calculation of the absorption maximum for infinite conjugation. In the case of polyene hydrocarbons, this band would be expected to be at 608 nm.

So far, only the main absorption band ( $\lambda_1$ ) and the *cis* peak ( $\lambda_2$ ) have been discussed. Further peaks are observed, however, when the conjugated chain is extended beyond the normal polyene skeleton. Figure 13 shows the spectra of decapreno- and dodecapreno- $\beta$ -carotene with 2 and 4 additional isoprene units. Apart from the quite unexpected loss of fine structure, a number of additional absorption bands can be seen ( $\lambda_3$ ,  $\lambda_4$ , etc.). The  $\lambda_1$  band is due to an electronic transition from the highest occupied to the lowest unoccupied  $\pi$ -orbital. It has been argued that the minor bands are overtones: i.e. transitions to higher unoccupied orbitals<sup>8</sup>. These overtone

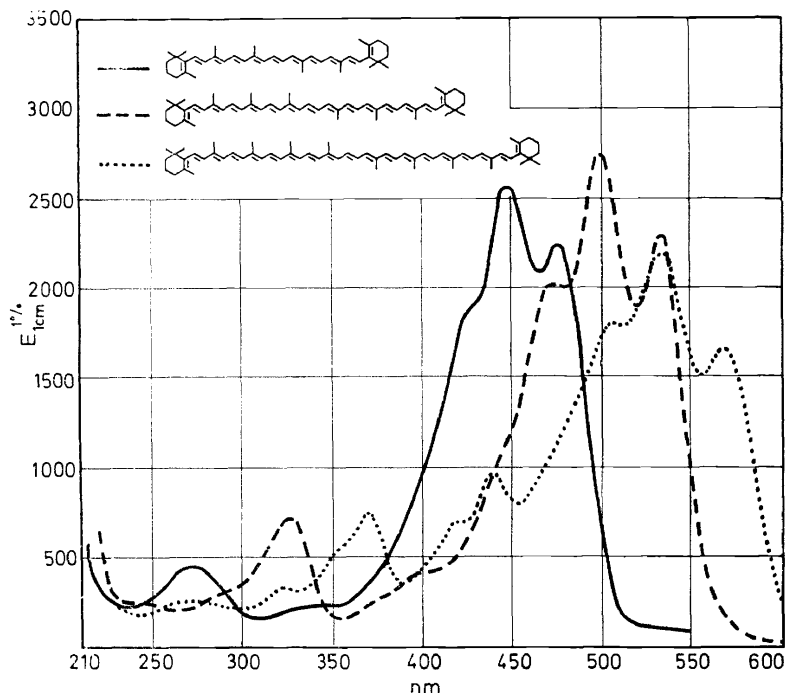


Figure 13. Ultraviolet and visible light absorption spectra of  $\beta$ -carotene (—), decapreno- $\beta$ -carotene (---) and dodecapreno- $\beta$ -carotene (····) (in petroleum ether).

bands can easily be calculated, because in an aliphatic polyene with  $n$  conjugated double bonds, the maximum of the  $\lambda_x$  band will lie very close to the maximum of a corresponding polyene with  $n/x$  double bonds. The  $\lambda_2$  band therefore corresponds to  $n/2$ ,  $\lambda_3$  to  $n/3$  etc.

The calculation, which is best carried out graphically, is exemplified in Figure 14.

The wave length maxima of the three peaks of the main absorption band are plotted against the number of double bonds. The curve has been extended beyond the one published<sup>8</sup> by using the data for decapreno- and dodecapreno- $\beta$ -carotene, taking into consideration the relatively small bathochromic influence of the two  $\beta$ -end groups (i.e. 14 effective double bonds

instead of 15, and 18 instead of 19, respectively). The  $\lambda_2$  peak for doccapreno- $\beta$ -carotene is then at  $n = 18/2 = 9$ ,  $\lambda_8$ :  $n = 6$ , etc. The calculated and observed values are indicated in the figure. The  $\lambda_2$  band or the first overtone represents a transition, which according to Dale<sup>8</sup>, is forbidden in linear all-*trans* compounds, but is allowed in angular shaped molecules, such as *cis* isomers. For linear, one-dimensional all-*trans* compounds only bands of odd order represent allowed transitions, while two-dimensional *cis* isomers show bands of odd and even order.

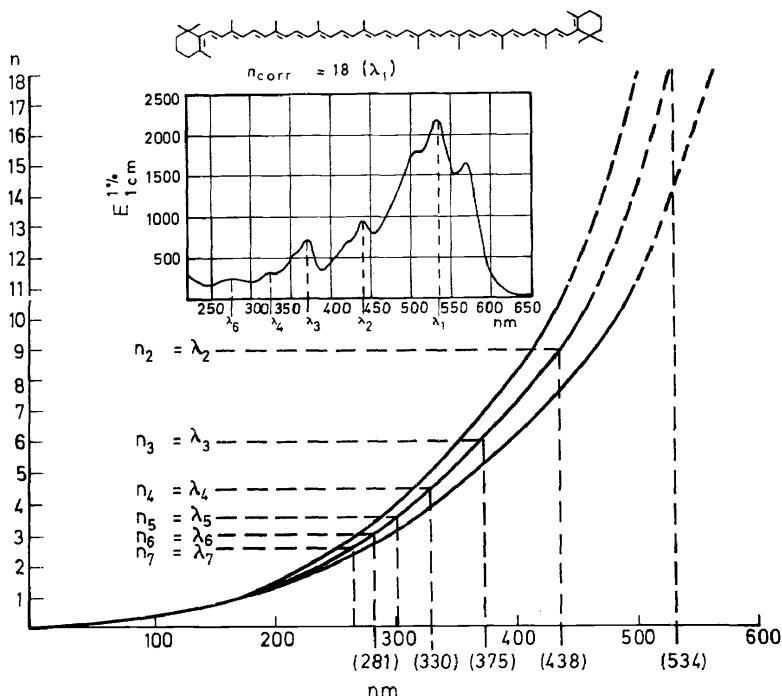


Figure 14. Graphic calculation of the overtone bands of dodecapreno- $\beta$ -carotene (in petroleum ether) according to Dale<sup>8</sup>.

An occasional observation of a  $\lambda_2$  band in all-*trans* polyenes has been explained by isomerisation in solution, but it might be argued that an *s-cis* conformation of the ring—as observed in X-ray studies—arranges the molecule in a two-dimensional structure, an argument similar to the one that has been used to explain the subsidiary maxima of vitamin A<sub>2</sub><sup>8</sup>.

### INFRARED SPECTROSCOPY

This technique has never played a major role in carotenoid chemistry, mainly due to the fact that the conjugated polyene system gives rise to only very weak bands. The development of more useful methods such as p.m.r. or mass spectroscopy has decreased its importance even more. However, very little material (0.2–1 mg.) is needed and i.r. spectroscopy is therefore used regularly. It has proved to be of value for the detection of

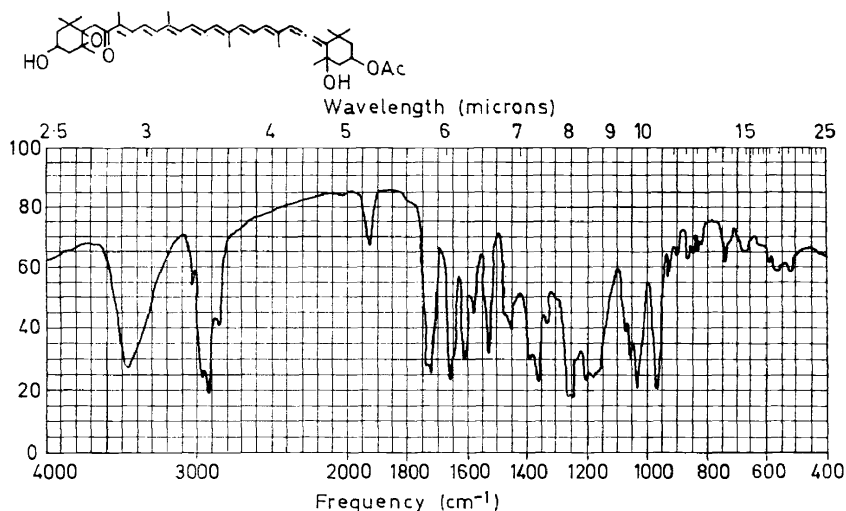


Figure 15. Infra-red absorption spectrum of fucoxanthin (KBr pellet).

certain special structural features, especially for hydroxyl, acetylenic, allenic and unreactive keto groups, e.g. like those in fucoxanthin and capsanthin.

Recently the structures of allenic and acetylenic carotenoids were solved with the help of i.r. spectroscopy<sup>9,10</sup>. The unusual peak at 1956 cm<sup>-1</sup> of fucoxanthin (Figure 15) could be assigned to an allenic group. The weak band at 2170 cm<sup>-1</sup> in alloxanthin (Figure 16) is characteristic for a disubstituted acetylene.

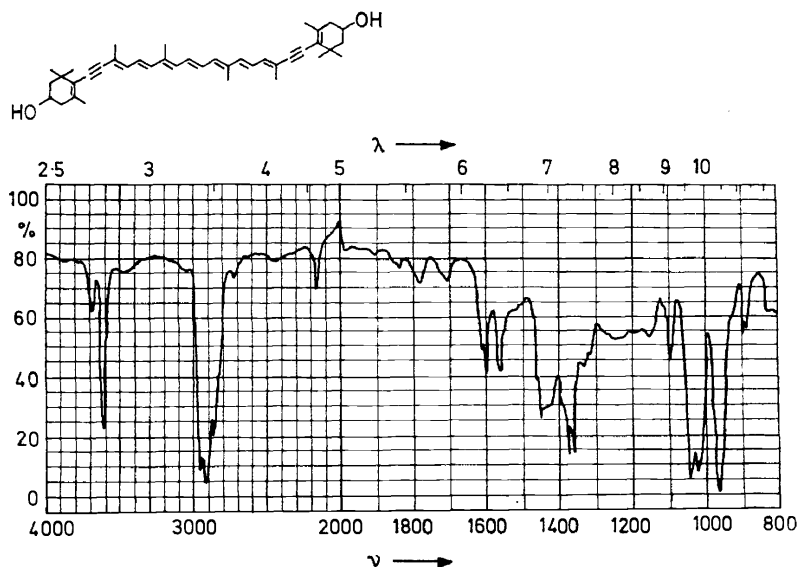


Figure 16. Infra-red absorption spectrum of alloxanthin (in CHCl<sub>3</sub>).



All carotenoids show a strong band near  $965\text{ cm}^{-1}$  due to C-H out-of-plane deformations of *trans* disubstituted ethylene groupings<sup>11</sup>. For all-*trans* carotenes this is a sharp singlet; *retro*-Carotenoids as well as some carbonyl-substituted or *cis* polyenes show a doublet in this region. This double peak seems to be conclusive for the *retro*-system<sup>12</sup>. In *retro*-apocarotenoids the

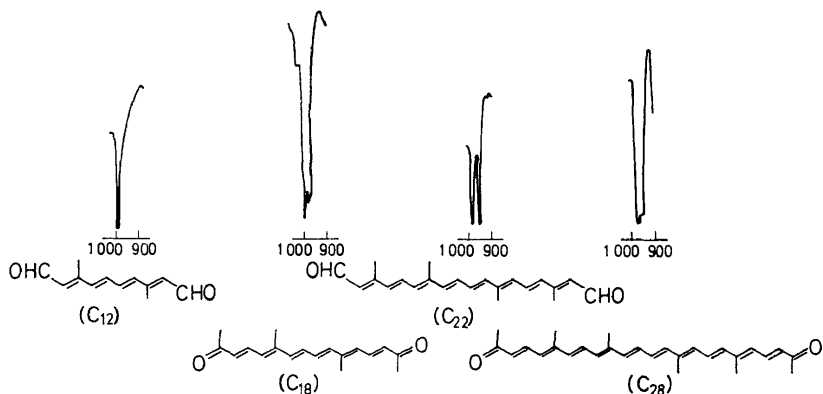


Figure 17. Infra-red absorption bands for apo-*retro*-carotenoids (KBr pellet).

appearance of this doublet seems to be dependent on the chain length as seen in Figure 17. The  $C_{12}$ -compound exhibits only a single peak, while the higher vinylogues show the characteristic pattern<sup>13</sup>.

### MOLECULAR STRUCTURE

Vitamin A intermediates, vitamin A acid and carotenoids have been examined by X-ray crystallography<sup>14</sup>. The results of these investigations are of great interest for the understanding of some unusual features of polyene spectroscopy.

Despite earlier predictions of a rapid convergence of the bond lengths of conjugated systems to a mean value on increasing chain length<sup>15</sup>, an alternation of shorter and longer bonds has been found. There is little sign of bonds of mixed nature. Only a small, but systematic decrease in the alternative character of the single and double bonds towards the centre of the molecule has been observed<sup>14d,f,h</sup>.

The chain is appreciably curved in its plane. This results from interactions of the chain methyl groups with their allylic hydrogen neighbours. The interaction causes a significantly smaller bond angle opposite the side chain methyl groups and from this follows the typical s-shaped bending of the chain as seen in Figure 18.

Furthermore, steric hindrance between the methyl groups of the ring and the hydrogen atoms on C-7 and C-8 is released by a rotation of  $40\text{--}50^\circ$  about the C-6—C-7 single bond. This explains the observed small contribution of a  $\beta$ -end group to the absorption spectrum, because the non-planar

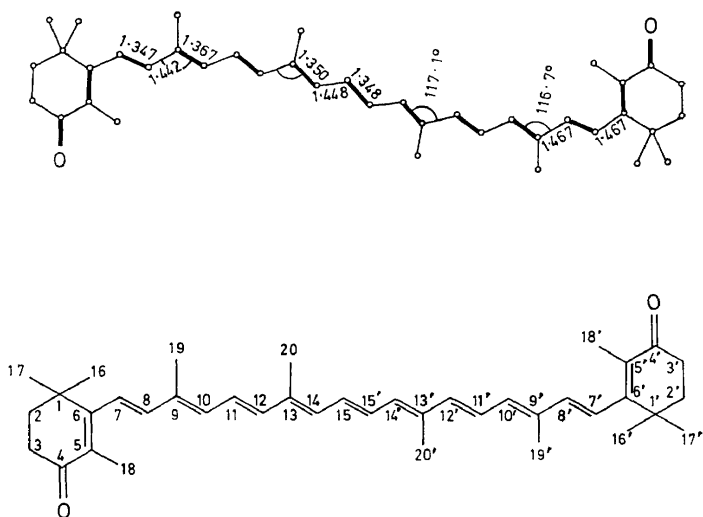


Figure 18. Formula and molecular structure of canthaxanthin.

structure limits overlap of the  $\pi$ -orbitals of the ring and the chain. With the exception of *trans*- $\beta$ -jonylideneacetic acid<sup>14a</sup>, which is *s-trans*, all compounds have the *s-cis* conformation of the  $\beta$ -end group. However, the rotation of the ring is about  $80^\circ$ <sup>14b</sup> in the case of a 9-*cis* isomer, indicating an additional steric hindrance between the hydrogen atoms at C-8 and C-11. This type of hindrance, which was first discussed by Pauling<sup>16</sup>, is indicated in Figure 19 for vitamin A isomers.

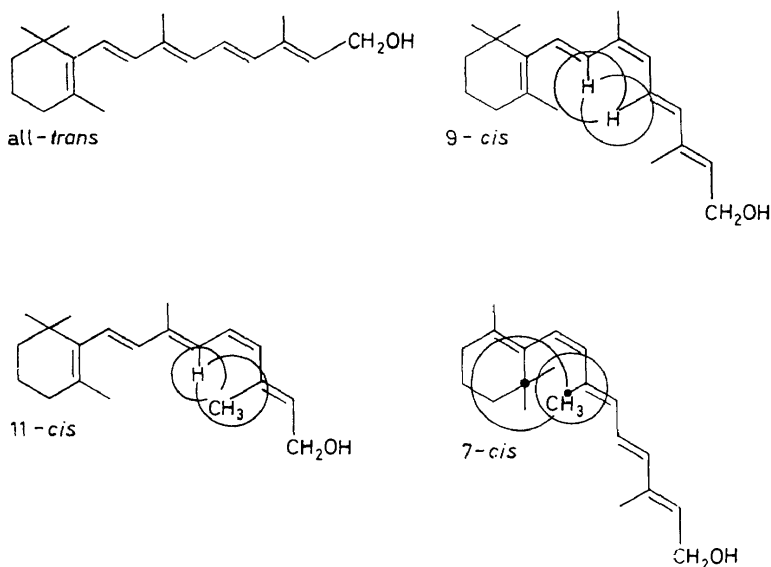


Figure 19. Pauling hindrance<sup>16</sup> of vitamin A isomers.

Overlap of substituents in the 1,4-position of the polyene chain tends to favour isomerization to the *trans* configuration. 9-*cis*-vitamin A has hydrogen atoms as the 1,4 substituents and is a very stable compound, although the X-ray studies indicate a non-planar arrangement of the chain about the C-8—C-9 single bond due to this interaction<sup>14b</sup>. 11-*cis*-vitamin A has been prepared. The 1,4 interaction of a hydrogen atom with a methyl group leads, however, to extremely easy isomerization. It has been argued, therefore, that a 7-*cis* isomer with a methyl group in the 1 and a large substituent in the 4-position of the *cis* bond would be too labile to exist under normal conditions.

### OPTICAL ROTARY DISPERSION (o.r.d.)

Some characteristic chiral end groups are shown in the *Figure 20*. O.r.d. curves of a number of carotenoids have been measured and a possible biogenetic interrelationship seems to emerge from these highly interesting studies<sup>9</sup>. The strong absorption makes o.r.d. measurements very difficult in the region of the main absorption band. A normal optical rotation curve with a Cotton effect at the same wavelength as the absorption maximum and a maximum molar rotation of 3000 has recently been reported for

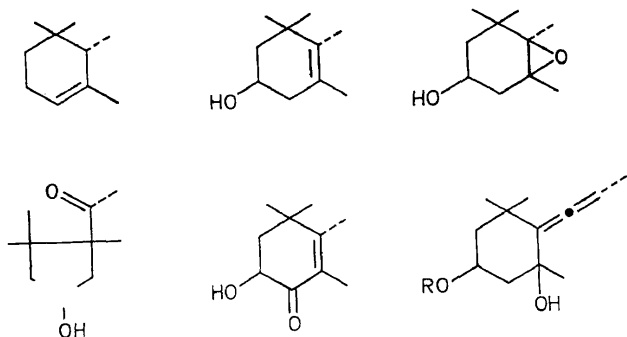


Figure 20. Typical chiral end groups of carotenoids.

astaxanthin<sup>17</sup>. Earlier curves were made mostly in dioxan solutions at 200–400 nm where, with the exception of possible *cis* peaks, carotenoids have maxima of comparatively low intensity only.

### PROTON MAGNETIC RESONANCE SPECTROSCOPY

Proton magnetic resonance (p.m.r.) spectroscopy, a technique complementary to the ones already discussed, was first used for carotenoid research by Jackman and Weedon in 1960<sup>18</sup>. Since that time its application has been reported in an ever-increasing number of papers in the literature, clearly demonstrating that p.m.r. is an important tool for the elucidation of structures in carotenoid chemistry. This is due to the fact that the chemical shifts of the signals as well as the magnitude of their splittings caused by

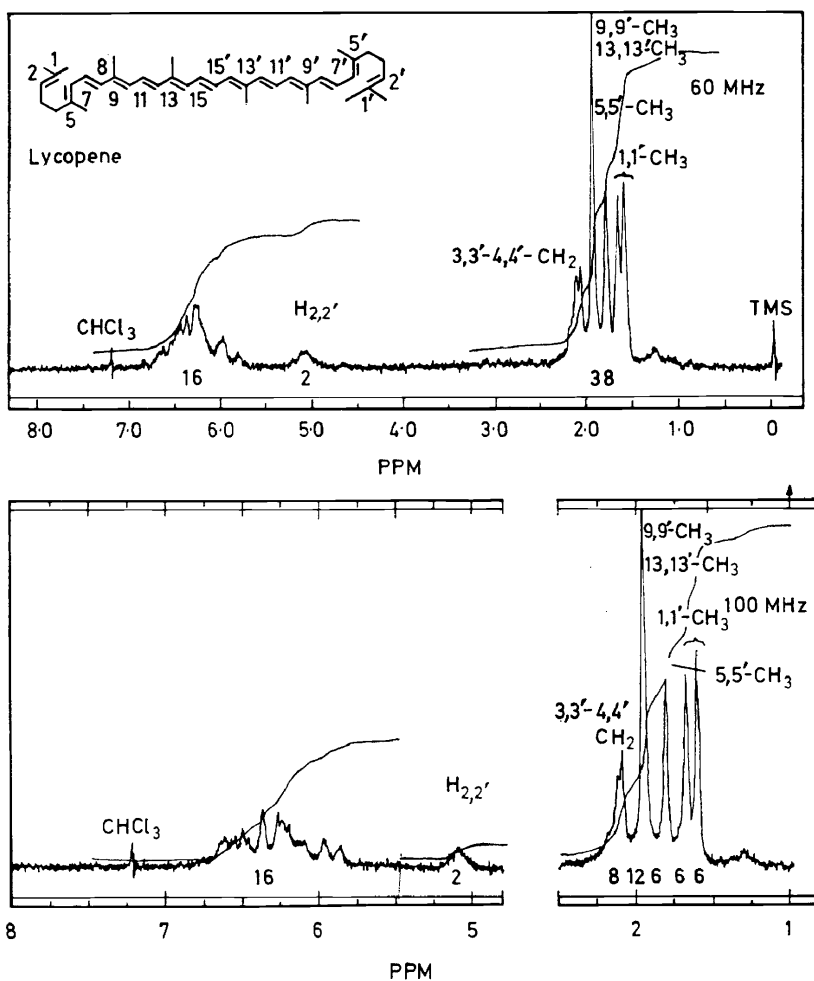
mutual spin-spin coupling of the protons directly reflect the structural features at different sites within a molecule.

Frequently, information on molecular structures was derived solely from the high-field part of the spectra between about 1 and 2.5 ppm. Especially the signals of the different methyl protons appearing mostly as singlets were found to be very useful for this purpose<sup>10, 19, 24</sup>. The low-field part of the spectrum between 5 and 6.5 ppm, on the other hand, arising from the majority of the olefinic protons, was often very little informative due to its complexity. This is caused by the near-coincidence of most of the chemical shifts resulting in strongly overlapping signals and hence in the existence of a complex jumble if measured at 60 or even at 100 MHz. Only few olefinic protons may be detectable outside this region, namely protons on isolated double bonds, protons at the end of a conjugated double bond system or protons being in the vicinity of a functional group with strong diamagnetic anisotropy, e.g. carbonyl or carboxyl groups.

The difficulties in the interpretation of the very complex pattern of the olefinic signals could be alleviated by a further increase of the spectrometer frequency, because this leads to a corresponding increase of the chemical shift differences and hence to a simplification of the analysis of the spectra.

An important progress in this connection has been achieved by the introduction of high-resolution p.m.r. spectrometers using superconducting magnets of high magnetic field strength. For more than a year we have been using such an instrument, namely a Varian 220 MHz spectrometer operating at a magnetic field strength of about 52,000 gauss. With the aid of this instrument we have studied, among others, the p.m.r. spectra of about 70 polyenes. We have found that the increase in chemical shift differences by a factor of 2.2 compared to 100 MHz instruments is actually in many cases sufficient to resolve the olefinic portion of the spectrum into more or less separated singlets or multiplets. Thus, it became possible even in rather complicated cases to deduce from the spectra chemical shifts and spin couplings of most or even all the olefinic protons and to apply these data to the elucidation of unknown structures. The drastic simplification of the spectra due to the increase in spectrometer frequency will be seen in the following examples.

In *Figure 21* we present the p.m.r. spectra of lycopene in  $\text{CDCl}_3$  solution. Because of the molecular symmetry the spectrum is expected to be relatively simple. A comparison of the 60- and 100 MHz spectra (first and second) shows that the former already reveals all spectral subtleties of the aliphatic part of the spectrum, whereas in the olefinic part the signals of only 2 of a total of 18 protons (H-2 and H-2' at about 5.1 ppm) can be identified. All other olefinic protons give rise to the complex pattern between 5.8 and 6.8 ppm. The situation is completely different in the third spectrum presenting the olefinic part measured at 220 MHz. Here almost all the signals are identified as doublets, triplets, or quartets and the approximate shifts of the signals of the central 4 protons, i.e. of H-14,14' and H-15,15', are deduced from a consideration of the signal areas. Their identification could be easily achieved from the last spectrum showing the same spectral range for the 15,15'-D<sub>2</sub>-compound. Here the 15,15'-proton signals have disappeared and the signals of H-14 and H-14' appear as a slightly broadened singlet.



(a)  
Figure 21

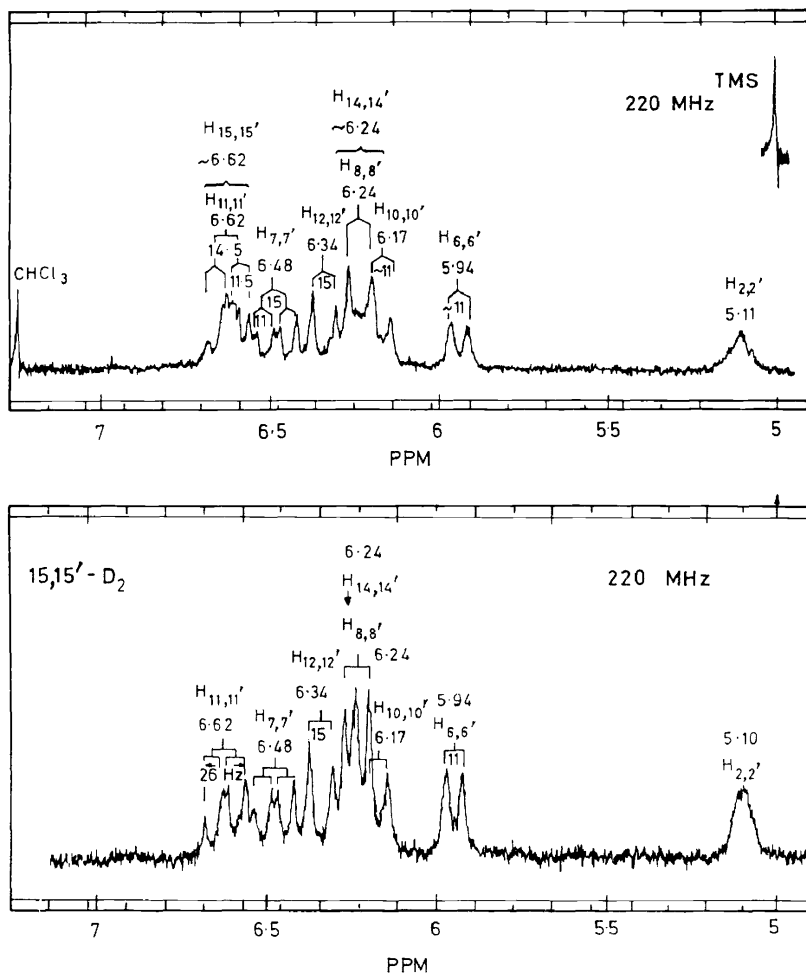


Figure 21. Proton magnetic resonance spectrum at 60 and 100 MHz (a) in comparison to the olefinic region at 220 MHz (b) of all-trans-lycopene and all-trans-15,15'-D<sub>2</sub>-lycopene (in CDCl<sub>3</sub>).

It should be pointed out that not only in this case but also with the other spectra discussed later on, a more or less complete assignment of the signals to the individual protons has been achieved. These assignments which might in a few cases be only tentative cannot be justified here in full detail. It should only be mentioned that they are based on one or more of the following arguments and techniques: comparison of chemical shifts and spin couplings in related molecules, starting with relatively simple ones; consideration of the signal intensities and their changes upon variation of spectrometer frequency; study of solvent effects; 100 MHz spin decoupling or tickling experiments. In some cases replacement of hydrogen by deuterium at specific positions was used for the identification of some of the protons, as for instance in the case of lycopene.

In *Figure 22*, as a further example, the 100 MHz spectrum of anhydro-vitamin A is shown in comparison with the olefinic region of the 220 MHz spectrum. Although the molecule is of rather low molecular weight the olefinic part of the 100 MHz spectrum is completely obscured because of the overlap of most of the signals. In the 220 MHz spectrum all individual doublets and quartets to be expected from this molecule of known structure are easily recognized and assigned to the different protons. The assignments were based here on the expected multiplet structures and spin couplings. Some of the olefinic protons have a small allylic coupling of about 1.4 Hz with their neighbouring methyl protons. Although this coupling is not resolved at 220 MHz the resulting broadening of the lines helps their identification.

The spectra of vitamin A and related compounds are generally rather simple at 220 MHz. Since a number of such spectra has been discussed very recently<sup>20</sup>, we summarize the chemical shifts and spin couplings of these compounds in *Table 4* (solvent  $\text{CDCl}_3$ ).

A comparison of the chemical shift data of selected protons of the *trans*- and the different *cis*-isomers indicates, that larger shift changes only occur for such protons being attached to, or in close geometrical proximity with, the corresponding *cis*-bond. This fact considerably simplifies the assignment of the signals of all the other protons in complicated spectra since the variation of their chemical shifts is in general rather small. On the other hand, the magnitude of the shift differences of protons at or near to the *cis*-bond is characteristic for its position in the molecule.

These shift differences (in ppm) between the different *cis*-isomers and their parent all-*trans* compounds are summarised in *Table 5*. Differences of less than 0.05 ppm have been omitted since they are thought not to be significant. Positive numbers indicate that the corresponding proton signals appear at lower magnetic field.

The different isomers can be distinguished from each other by the shift changes of some of the proton signals compared with the all-*trans* compound. A significant shift of the signal of H-8, e.g. is only observed for 9-*cis* isomers. The signal of H-10 is only shifted downfield in the case of the 11-*cis* compound. These and additional experimental rules derived from the data presented in *Tables 4* and *5* have been found to be extremely useful for the elucidation of the structures of several *cis*-isomeric carotenoids as will be shown later.

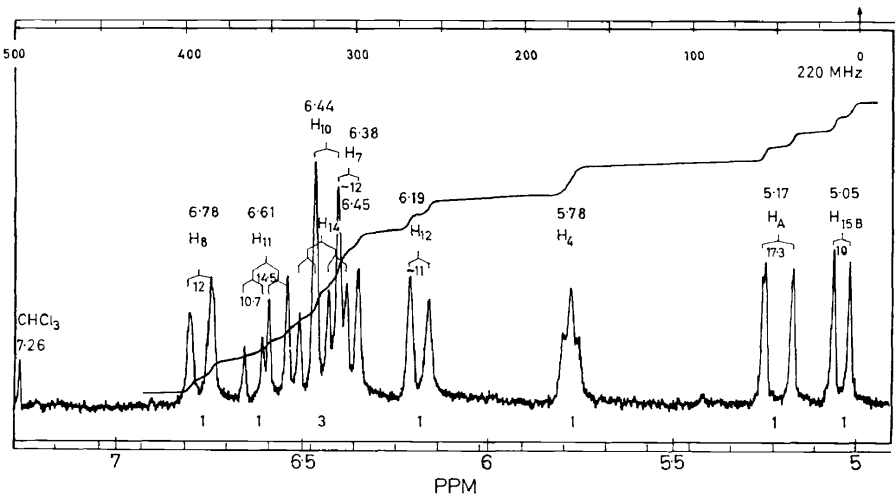
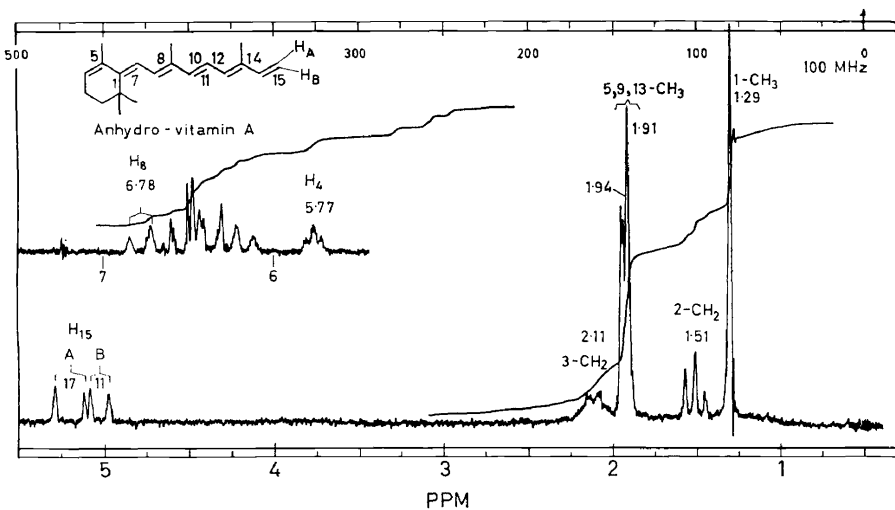


Figure 22. 100 and 220 MHz proton magnetic resonance spectra of anhydro-vitamin A (in CDCl<sub>3</sub>).

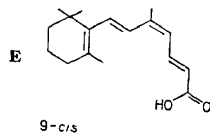
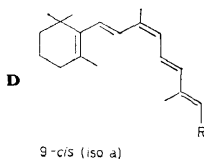
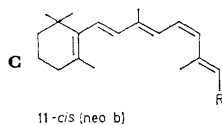
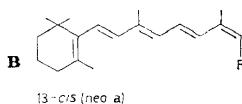
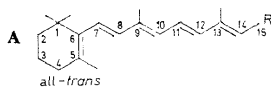


Table 4. Proton magnetic resonance data of vitamin A

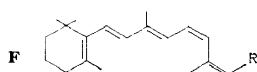
Compound	R	Olefinic hydrogens (ppm)									CH <sub>3</sub>	
		4	7	8	10	11	12	14	15		1	5
<b>A</b>	CH <sub>2</sub> OH	—	6·14	6·09	6·08	6·60	6·27	5·67	—		1·03	1·72
	CH <sub>2</sub> OCH <sub>3</sub>	—	6·14	6·09	6·09	6·60	6·29	5·62	—		1·03	1·71
	CH <sub>2</sub> OCOCH <sub>3</sub>	—	6·19	6·10	6·10	6·65	6·28	5·61	—		1·03	1·71
	CHO	—	6·35	6·17	6·19	7·15	6·37	5·97	—		1·03	1·72
	COOH	—	6·29	6·14	6·15	7·03	6·31	5·79	—		1·02	1·72
	COOCH <sub>3</sub>	—	~6·27	~6·11	6·13	6·99	6·27	5·79	—		1·02	1·71
	CH <sub>3</sub>	—	~6·11	~6·11	6·08	6·47	6·27	5·59	—		1·03	1·71
<b>B</b>	CH <sub>2</sub> OH	—	6·17	6·10	6·13	~6·65	~6·60	5·55	—		1·03	1·71
	CH <sub>2</sub> OCOCH <sub>3</sub>	—	6·17	6·10	6·12	6·69	6·59	5·47	—		1·02	1·70
	CHO	—	6·36	6·18	6·24	7·04	7·30	5·85	—		1·04	1·73
	COOH	—	6·29	6·17	6·29	7·03	7·77	5·69	—		1·03	1·72
<b>C</b>	CH <sub>2</sub> OCOCH <sub>3</sub>	—	6·20	6·12	6·56	6·39	5·87	5·63	—		1·02	1·71
	CHO*	—	6·32	6·14	6·54	6·69	5·92	6·07	—		1·02	1·71
	COOH	—	6·28	6·14	6·52	6·60	5·91	5·90	—		1·03	1·72
<b>D</b>	CHO*	—	6·31	6·64	6·06	7·20	6·27	5·94	—		1·05	1·75
	COOH	—	6·31	6·67	6·09	7·15	6·27	5·82	—		1·04	1·75
<b>E</b>	—	—	6·39	6·73	6·10	7·89	5·82	—	—		1·03	1·73
<b>F</b>	CH <sub>2</sub> OH	—	6·16	6·09	6·05	6·45	5·86	5·54	—		1·01	1·69
	CH <sub>2</sub> OCOCH <sub>3</sub>	—	6·19	6·08	6·09	6·49	5·87	5·49	—		1·01	1·70
	CHO*	—	6·28	6·08	6·20	6·77	6·11	5·98	—			
<b>G</b>	CHO*	—	6·36	6·68	6·16	7·16	7·25	5·87	—		1·01	1·68
	COOH	—	6·27	6·64	6·18	7·11	7·68	5·66	—		1·05	1·77
<b>H</b>	—	5·73	6·14	6·65	—	—	—	—	—		1·27	1·86
<b>I</b>	OCOCH <sub>3</sub>	5·76	6·36	6·72	6·30	6·45	6·04	—	—		1·29	1·86
<b>J</b>	—	5·78	6·38	6·78	6·44	6·61	6·19	6·45	A5.17 B5.05		1·29	~1·91†

\*D. J. Patel, *Nature* **221** 925 (1969). n.o. = not observed; n.g. = not given.

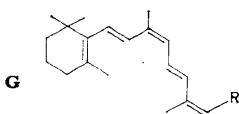
†Assignment uncertain.



CH <sub>3</sub> (cont.)		CH <sub>2</sub>				functional groups	coupling constants (J in Hz)				
9	13	2	3	4	15		2,3	7,8	10,11	11,12	14,15
1.97	1.85	~1.47	~1.61	2.02	4.29	OCH <sub>3</sub> : 3.37 OAc: 2.05 CHO: 10.09 COOH: n.o. COOCH <sub>3</sub> : 3.70 14CH <sub>3</sub> : 1.76 (J = 6.7 Hz)	—	±0.3	±0.5	±0.3	±0.3
1.95	1.85	~1.47	~1.61	2.01	4.08		—	~16	11.0	14.8	6.8
1.96	1.89	~1.46	~1.61	2.02	4.72		—	~16	11.0	15.0	6.8
2.03	2.32	~1.46	~1.62	~2.0	—		—	~16.0	11.3	15.0	7.0
2.01	2.37	~1.47	~1.62	~2.02	—		—	16.0	11.5	15.0	8.3
2.01	2.36	~1.45	~1.61	~2.01	—		—	16.0	11.5	15.0	—
1.95	1.81	~1.46	~1.62	2.01	—	OAc: 2.05 CHO: 10.21 COOH: ~9.9	—	n.o.	11.0	15.0	—
1.96	1.93	~1.47	~1.61	~2.03	4.30		—	~16	n.o.	~15	7.0
1.96	~1.95	~1.44	~1.59	~2.01	4.74		—	16.0	~10.5	~14.5	7.0
2.03	2.15	~1.47	~1.63	~2.0	—		—	16.0	11.0	15.0	8.0
2.00	2.10	~1.46	~1.63	~2.0	—	OAc: 2.06 CHO: 10.10 COOH: n.o.	—	16.0	11.5	15.0	—
1.93	1.92	~1.46	~1.61	~2.01	4.71		—	~16	11.8	11.5	7.0
1.99	2.36	n.g.	n.g.	n.g.	—		—	16.0	11.5	13.0	8.0
1.98	2.36	~1.45	~1.62	2.02	—		—	16.0	~11.5	~11.5	—
2.00	2.30	n.g.	n.g.	n.g.	—	CHO: 10.07 COOH: n.o.	—	15.9	11.8	15.4	8.2
2.01	2.37	~1.48	~1.64	~2.04	—		—	15.7	11.3	14.7	—
2.04	—	~1.47	~1.63	~2.04	—	COOH: ~10.5	—	15.7	11.7	15.0	—
1.92	1.87	~1.43	~1.58	~2.0	4.04	OAc: 2.02 CHO: 9.71	—	16.0	~11.7	~11.3	6.8
1.93	1.89	~1.45	~1.59	~2.0	4.50		—	16.0	n.o.	~11	7.0
1.96	2.07	n.g.	n.g.	n.g.	—	CHO: 10.27 COOH: n.o.	—	16.0	12.5	11.8	8.1
2.05	2.15	n.g.	n.g.	n.g.	—		—	16.0	10.5	15.0	8.0
2.02	2.10	~1.48	~1.65	~2.05	—	—CH <sub>2</sub> —COOH 3.23 ~9.8	—	15.7	11.5	15.0	—
1.95	—	1.48	2.09	—	—		6.2	11.7	—	—	—
~1.93†	1.91†	1.50	2.10	—	4.17	14CH <sub>3</sub> : 2.54 OAc: 2.01	6.2	12.0	15.0	10.5	—
1.94†	~1.91†	1.49	2.09	—	—		6.2	12.0	~14.5	10.7	A~17 B~10



11,13-di-cis (neo c)



9,13-di-cis (iso b)

retro compounds:

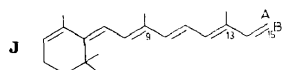
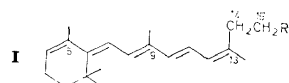
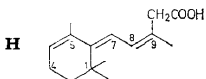
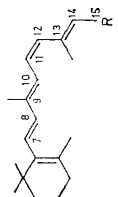
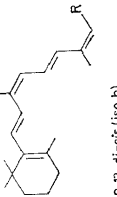
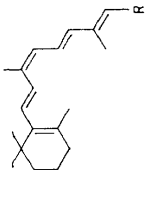


Table 5. Significant differences of chemical shifts ( $> 0.05$  ppm) of vitamin A and A<sub>2</sub> isomers in comparison with corresponding all-*trans* compounds.  
(in : CDCl<sub>3</sub>)

Compound	R	Olefinic hydrogens							CHO	CH <sub>3</sub>		CH <sub>2</sub>
		7	8	10	11	12	14	15		9	13	15
 11- <i>cis</i> (neo b)	-COOH -CHO -CH <sub>2</sub> OCOCH <sub>3</sub>	— — —	— — —	+0.37 +0.35 +0.46	-0.43 -0.46 -0.26	-0.40 -0.45 -0.41	+0.11 +0.10 —	— — —	— — —	— — —	— — —	— — —
	-CHO -CH <sub>2</sub> OH (Vitamin A <sub>2</sub> - CH <sub>2</sub> OH)	-0.07 — —	-0.09 — —	— — -0.06	-0.38 -0.15 -0.16	-0.26 -0.41 -0.42	— -0.13 -0.14	-0.38 — —	— — —	-0.07 — —	-0.25 — —	— -0.25 -0.21
	-COOH -CHO -CH <sub>2</sub> OH -CH <sub>2</sub> OCOCH <sub>3</sub> (Vitamin A <sub>2</sub> - CH <sub>2</sub> OPAB)	— — — — —	— — — — —	+0.14 — — — —	— -0.11 — — —	+1.46 +0.93 +0.33 +0.31 +0.44	-0.10 -0.12 -0.12 -0.14 -0.06	— +0.12 — — —	— — — — —	— — — — —	-0.27 -0.17 +0.08 +0.06 —	— — — — n.o.
 9,13-di- <i>cis</i> (iso b)	-COOH -CHO	— —	+0.50 +0.51	— —	+0.08 —	+1.37 +0.88	-0.13 -0.10	— +0.18	— —	— —	-0.27 -0.17	— —
	-COOH -CHO (Vitamin A <sub>2</sub> - CH <sub>2</sub> OH)	— — —	+0.53 +0.47 +0.53	-0.06 -0.13 -0.11	+0.12 — +0.10	— -0.10 -0.07	— — —	— — —	— — —	— — —	— — —	— — —
	 9- <i>cis</i> (iso a)	— — —	— — —	— — —	— — —	— — —	— — —	— — —	— — —	— — —	— — —	— — —

As another example we present in *Figure 23* the 100 MHz spectrum and the olefinic range of 220 MHz of  $\beta$ -apo-12'-carotenal(C<sub>25</sub>) in CDCl<sub>3</sub>. Again the situation is similar: only the 220 MHz spectrum is completely analyzable because all signals are separately identified. Some characteristic features seen in this spectrum in common with all other spectra of related all-*trans* molecules, should be briefly mentioned: H-7 and H-8 normally give rise at about 6.1 to 6.2 ppm to a singlet or an AB-quartet with  $J_{7,8} \sim 16$  Hz and relatively small chemical shift differences. Therefore, the outer two lines may be very weak in intensity. All compounds with a  $\beta$ -end group have a slightly broader H-7 signal due to the long-range coupling of H-7 with the 5-methyl- and 4-methylene protons as is easily proven by 100 MHz decoupling experiments.

The doublets observed for H-10, H-12 and of H-14 are situated at relatively high magnetic fields, while the quartets of H-11, H-15 and H-15' with total splittings of about 26 Hz, as expected for the all-*trans* configuration, appear at relatively low magnetic fields. Other proton signals may be detected there if strong downfield shifts occur due to strongly anisotropic groups. This is true here for H-14' being in a *cis*-relationship to the carbonyl function.

We have studied the 220 MHz spectra of a number of  $\beta$ -apocarotenoids and their p.m.r. data are collected in *Table 6*. Whereas the structures of the all-*trans* compounds were well established the structures of some of their *cis* isomers included in *Table 6* have only been deduced during the course of this study. Of great help in this task was the fact that most of the signals of the *trans* compounds could be assigned. The observation of specific changes of the chemical shifts of the olefinic protons with the *cis* isomers facilitated the elucidation of their structure as will become evident by the following discussion.

In *Figure 24* the olefinic part of the 220 MHz spectrum of  $\beta$ -apo-12'-carotenal (C<sub>25</sub>) in CDCl<sub>3</sub> is repeated together with those of two *cis* isomers, which were isolated from the reaction mixture on partial hydrogenation of the 15,15'-dehydro-compound. These compounds are of orange and yellow colour. From a comparison of these spectra the structures of these isomers were easily deduced.

The second spectrum of *Figure 24* was obtained from the orange isomer. Here, the AB-pattern of H-7 and H-8 as well as the doublet of H-10 are detected at their expected positions around 6.1 ppm. The doublet ( $J = 12$  Hz) at very low magnetic field must be attributed to a proton close to a *cis* carbonyl, i.e. to H-14', additionally shifted downfield compared with the *trans*-compound. Although the chemical shift differences in the 100 MHz spectrum were very small, a spin decoupling experiment could be used to localize the signal of H-15'. Irradiation of the H-14'-doublet led to considerable changes around 6.4 ppm. Here the 220 MHz spectrum reveals a two proton signal, consisting of a doublet with a splitting of 15 Hz and a quasi-triplet with a total splitting of less than 23 Hz. From this follows that this quasi-triplet must be assigned to H-15' and that the compound must be the 15-*cis* isomer. On the basis of this assumption, all other signals can be assigned and it is seen that, compared to the all-*trans* compound, the signals of H-14 and H-14' are shifted downfield. The signals of H-15 and H-15' show an upfield shift as would be expected for the 15-*cis* configuration.

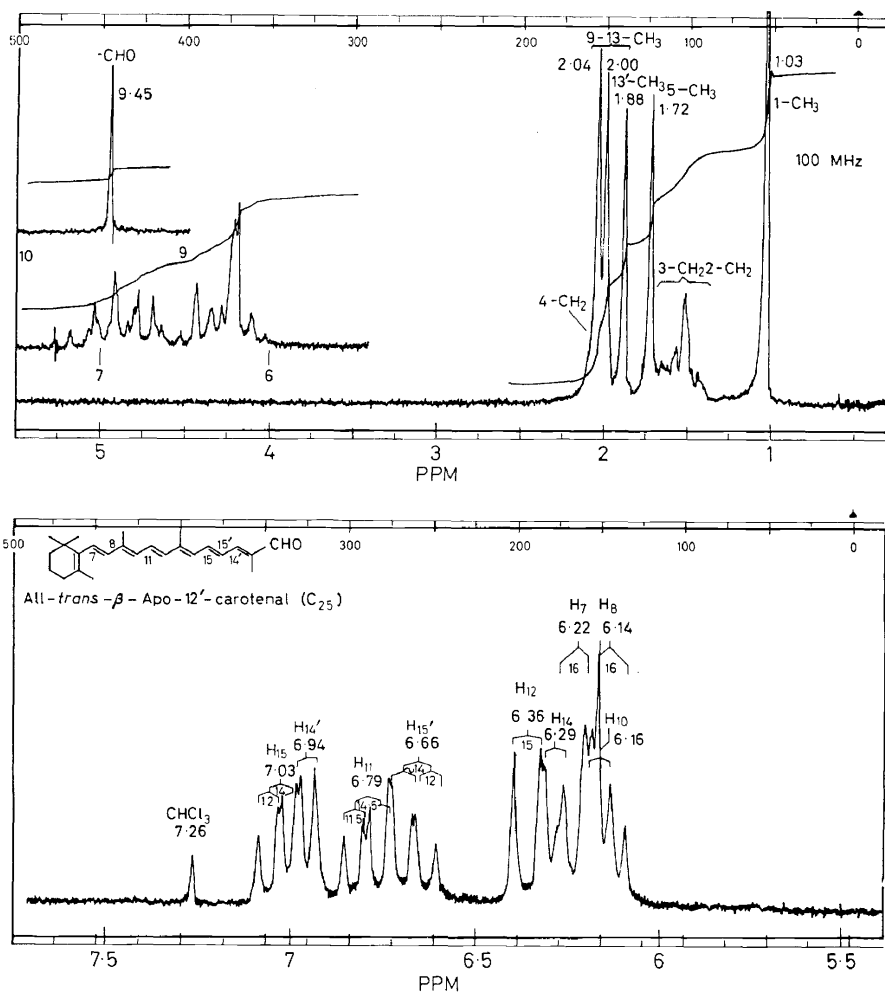


Figure 23. 100 and 220 MHz proton magnetic resonance spectrum of all-trans- $\beta$ -apo-12'-carotenal( $C_{25}$ ) (in  $CDCl_3$ ).

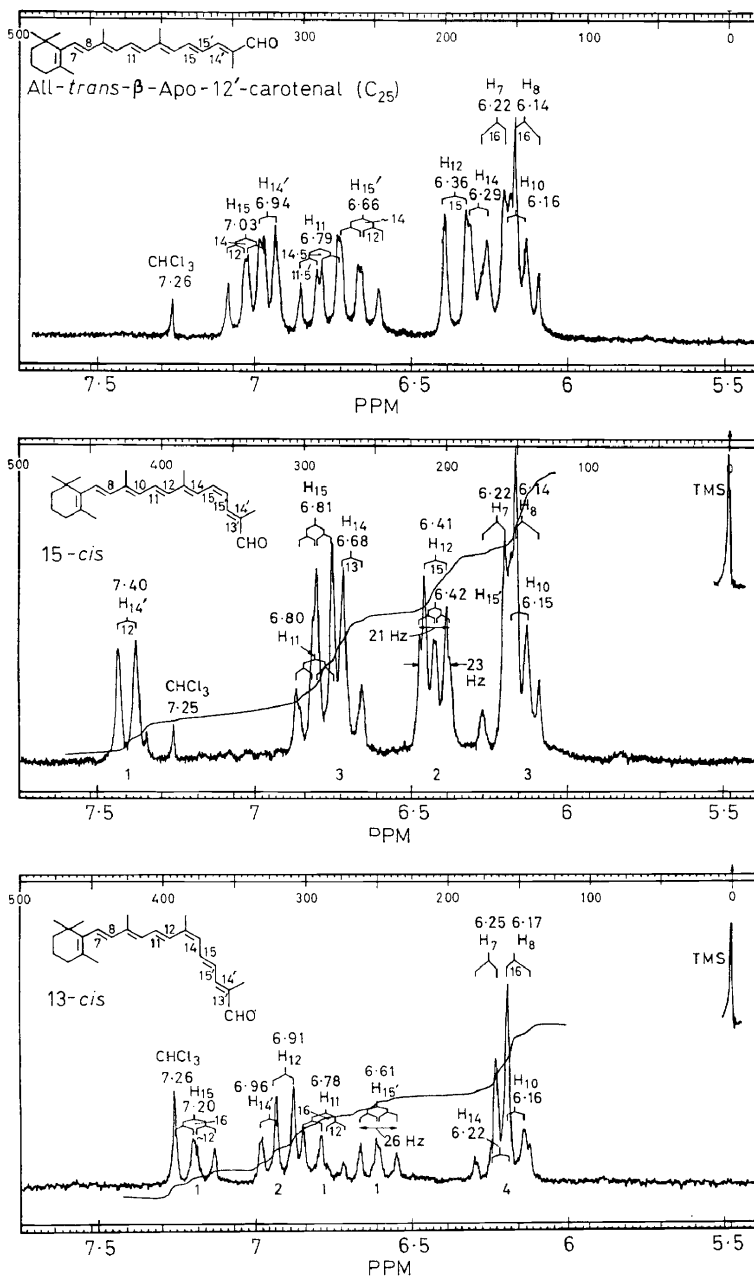


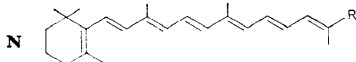
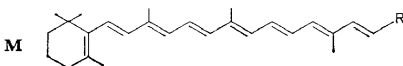
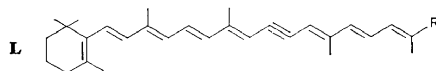
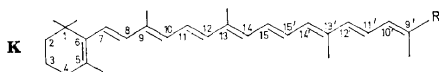
Figure 24. Olefinic part of the proton magnetic resonance spectrum (220 MHz) of all-*trans*-, 15-*cis*- and 13-*cis*-  $\beta$ -apo-12'-carotenol(C<sub>25</sub>) (in CDCl<sub>3</sub>).

Table 6. Proton magnetic resonance

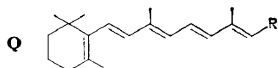
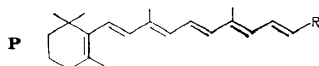
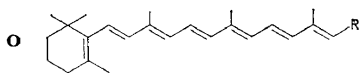
Compound	R	Olefinic hydrogens (ppm)								
		7	8	10	10'	11	11'	12	12'	13'
<b>K</b>	CHO	6·20	6·14	6·14	6·94	~6·70†	6·62	6·38	6·73	—
	CH <sub>2</sub> OCOCH <sub>3</sub>	~6·15	~6·15	~6·15	n.a.	6·65†	6·46†	n.a.	n.a.	—
	CHO (9-cis)	6·19	~6·66	6·05	6·93	6·81†	6·63	6·28	6·72	—
	COOCH <sub>3</sub>	6·18	6·14	6·14	n.a.	n.a.	n.a.	6·35	6·52	—
<b>L</b>	COOC <sub>2</sub> H <sub>5</sub>	6·23	6·14	6·14	7·27	6·75	~6·57	6·36	~6·63	—
	COOC <sub>2</sub> H <sub>5</sub> (9'-cis)	6·24	6·12	~6·13	6·51	6·74	7·47	6·36	6·45	—
<b>M</b>	CHO	6·20	6·14	6·15	—	6·74	~6·16	6·35	7·15	—
<b>N</b>	CHO	6·22	6·14	6·16	—	6·79	—	6·36	—	—
	CHO (15-cis)	6·22	6·14	6·15	—	6·80	—	6·41	—	—
	CHO (13-cis)	6·25	6·17	6·16	—	6·78	—	6·91	—	—
	CH <sub>2</sub> OCOCH <sub>3</sub>	6·18	6·12	6·13	—	6·64	—	6·32	—	—
<b>O</b>	COOCH <sub>3</sub>	6·24	6·14	6·16	—	6·74	—	6·31†	—	5·79
	COOH	6·22	6·15	6·15	—	6·75	—	6·32†	—	5·81
<b>P</b>	COOCH <sub>3</sub>	6·24	6·12	6·14	—	6·83	—	6·34	—	—
<b>Q</b>	COOCH <sub>3</sub>	6·27	6·11	6·13	—	6·99	—	6·27	—	—

For all compounds: 2-CH<sub>3</sub>-group      1·56 ± 0·01 ppm  
 3-CH<sub>3</sub>-group      1·62 ± 0·02 ppm  
 4-CH<sub>3</sub>-group      ~2·02 ± 0·04 ppm

†assignment uncertain  
 n.a. = not assigned



Olefine hydrogens (cont.)				CH <sub>3</sub>							functional groups
14	14'	15	15'	1	5	9	9'	13	13'	14'	
6.26	6.43†	6.77†	6.63	1.02	1.73	1.99†	1.90	2.01†	2.01†	—	CHO: 9.44
6.24	n.a.	~6.62†	~6.62†	1.03	1.73	1.98†	1.84	1.98†	1.95†	—	OAc: 2.09
6.24	6.43	6.76	6.61	1.04	1.75	~2.0	1.90	~2.0	~2.0	—	CHO: 9.44
6.24	n.a.	n.a.	n.a.	1.03	1.73	~2.0	~2.0	~2.0	~2.0	—	COOCH <sub>3</sub> : 3.76
											COOCH <sub>2</sub> : 4.23
5.73	5.87	—	—	1.02	1.72	2.00†	2.01†	2.11	2.11	—	CH <sub>3</sub> : 1.33
5.72	5.82	—	—	1.02	1.71	1.97†	2.00†	2.11	2.11	—	COOCH <sub>3</sub> : 4.25
											CH <sub>3</sub> : 1.34
6.27	n.a.	n.a.	n.a.	1.04	1.73	2.00†	—	2.03†	1.96†	—	CHO: 9.57
6.29	6.94	7.03	6.66	1.03	1.73	2.00†	—	2.02†	1.87	—	CHO: 9.45
6.68	7.40	6.81	6.42	1.04	1.73	2.01†	—	2.04†	1.89	—	CHO: 9.54
6.22	6.96	7.20	6.61	1.04	1.73	2.01†	—	2.06†	1.88	—	CHO: 9.46
~6.18	~6.18	6.60†	6.40†	1.03	1.72	1.97	—	1.97	1.82	—	OAc: 2.09
6.22	—	7.00	6.36†	1.03	1.72	2.00	—	2.03	—	2.36	COOCH <sub>3</sub> : 3.72
6.23	—	7.03	6.37†	1.03	1.72	1.99	—	2.03	—	2.36	
6.20	—	7.69	5.88	1.02	1.72	1.96	—	2.07	—	—	COOCH <sub>3</sub> : 3.76
5.79	—	—	—	1.02	1.71	2.01	—	2.36	—	—	COOCH <sub>3</sub> : 3.70





The last spectrum in *Figure 24* was obtained from the yellow isomer. Three quasi-triplets and quartets due to the protons H-11, H-15 and H-15' can be seen. All these signals have a total splitting of 26 to 28 Hz indicating an 11- and 15-*trans* configuration. The typical AB-pattern of H-7 and H-8 is at its regular position with  $J_{7,8}$  of about 16 Hz proving, that the 7,8- and 9,10-double bonds must also be *trans*. Therefore, only the possibilities of a 13-*cis*, 13'-*cis* or a 13,13'-di-*cis* isomer remain. The last two possibilities are excluded by the observation that the chemical shifts of the aldehyde proton (see below) as well as that of H-14' are the same as in the all-*trans* compound. The assumption of a 13-*cis* configuration is consistent with the predictable shift differences: compared to the all-*trans* compound the signals of H-12 and H-15 are shifted downfield, whereas the H-14 and H-15'-signals are slightly shifted upfield as would be expected.

A further convincing example for the capabilities of 220 MHz spectroscopy is given in *Figure 25* showing the olefinic range of the spectra of all-*trans*- $\beta$ -apo-8'-carotenal(C<sub>30</sub>) and of one of its *cis* isomers. Although these molecules contain 12 different olefinic protons absorbing in a range of less than 1 ppm, the doublets and quartets of all these protons can be recognized and in most cases unambiguously assigned to the different protons. Independently of the correctness of all the assignments the following observation led to the deduction of the unknown structure: a comparison of the two spectra indicates that the typical AB-pattern of H-7 and H-8 at about 6.2 ppm has now disappeared. Only the signal of one of these two protons, probably of H-7, is found at 6.19 ppm. The signal of H-8 is presumably located around 6.66 ppm, i.e. about 0.5 ppm downfield as compared to the all-*trans* compound. In agreement with this, the doublet observed at 6.05 ppm is assigned to H-10, now shifted slightly upfield, as is the case in 9-*cis* vitamin A compounds (see *Table 5*).

The spectra of ethyl all-*trans*-15,15'-dehydro- $\beta$ -apo-8'-carotenoate(C<sub>30</sub>) and of an unknown *cis* isomer are compared in *Figure 26*. The spectrum of the latter shows a quartet at very low field. The doublet of H-10' which occurred at 7.27 ppm with the *trans* compound is shifted upfield by as much as 0.76 ppm. This indicates that this isomer should have a 9'-*cis* configuration. On the basis of this assumption a complete assignment of all signals has been achieved leading to reasonable values for the shift differences between the spectrum of the all-*trans* and the 9'-*cis* compound.

In the preceding examples only the analysis of the olefinic part of the spectra could be used for the elucidation of the structures, because the shift differences observed with the signals of the methyl protons were rather small and the deduced information was therefore less reliable. This must, however, not be true in all cases.

The comparison of the chemical shifts of aldehydic protons, on the other hand, might also be useful in special cases for the deduction of molecular structures. This is demonstrated by the chemical shift data collected in *Table 7* for the aldehydic proton of conjugated aldehydes with a methyl group at the  $\alpha$ -carbon. A comparison of literature data and results from our own unpublished work for *cis*  $\beta$ -C<sub>14</sub>-aldehyde and 9'-*cis*-15,15'-dehydro- $\beta$ -apo-8'-carotenal(C<sub>30</sub>) indicates that the signals of the aldehydic proton of the *trans* compounds appear at considerably higher fields (9.2 to 9.7 ppm)

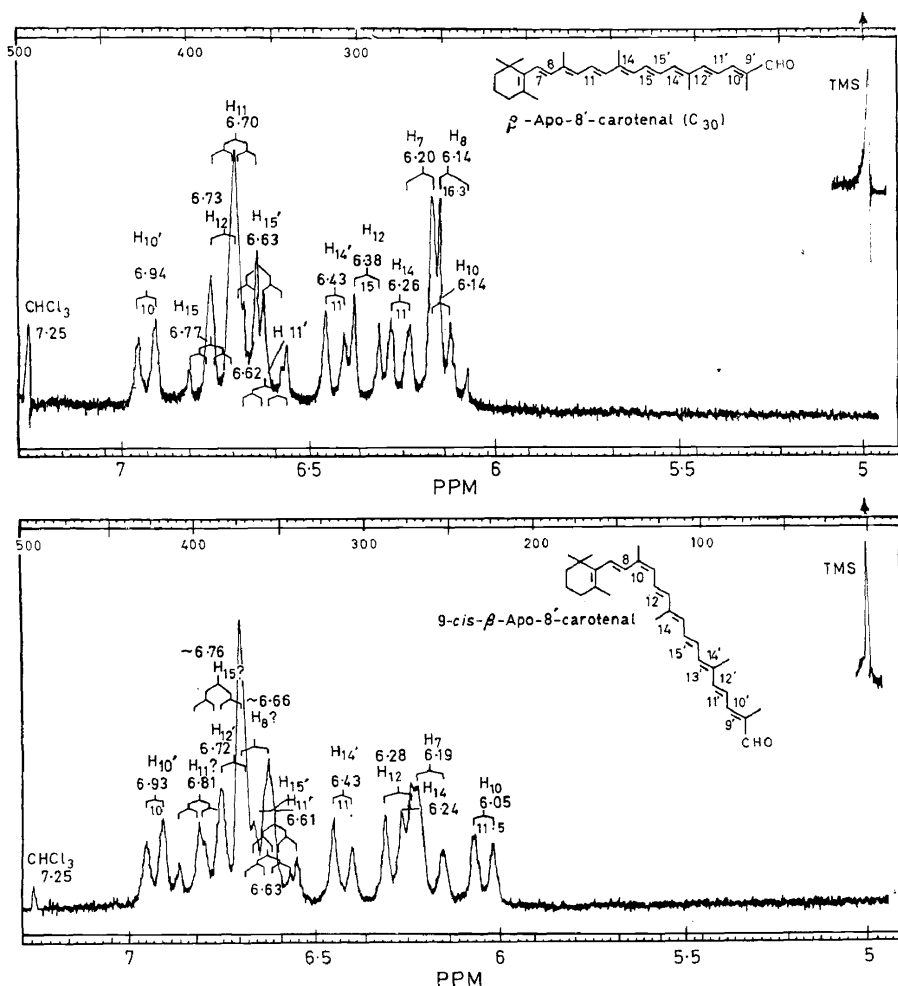


Figure 25. Olefinic part of the proton magnetic resonance spectrum (220 MHz) of all-trans- and 9-cis-β-apo-8'-carotenal(C<sub>30</sub>) (in CDCl<sub>3</sub>).

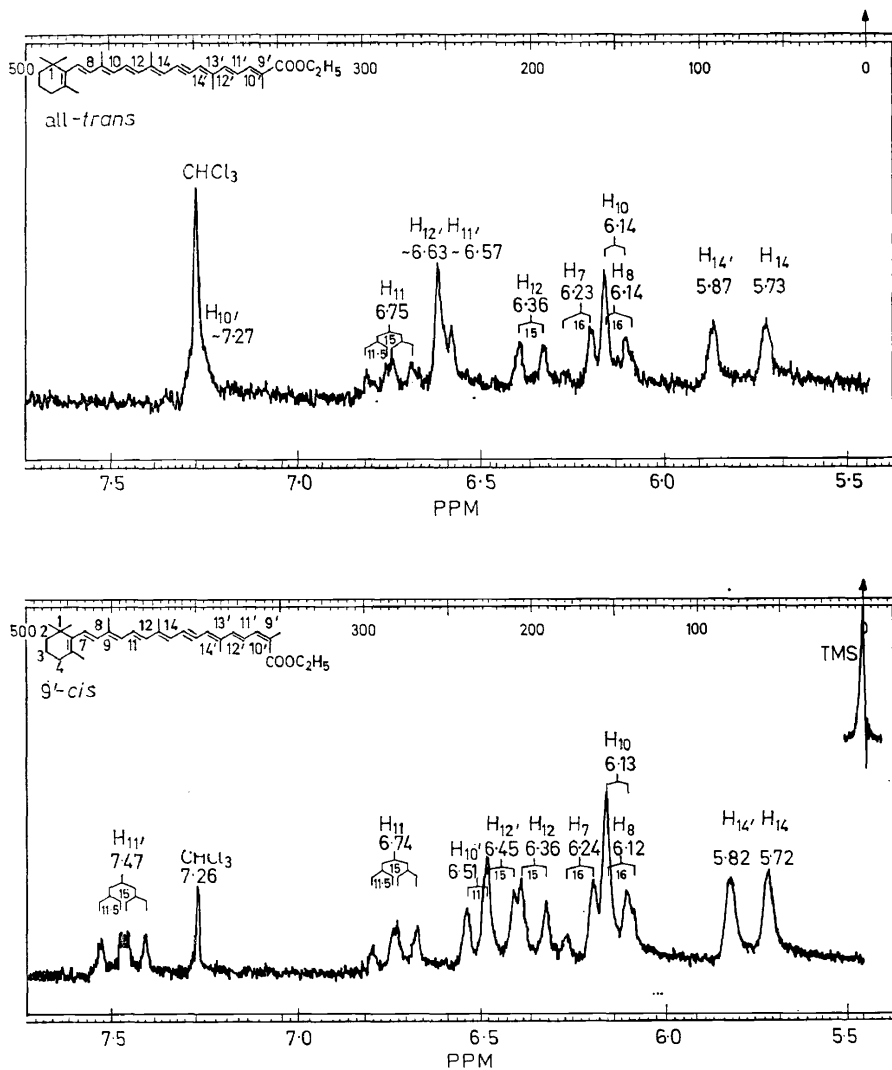


Figure 26. Olefinic part of the proton magnetic resonance spectrum (220 MHz) of all-*trans*- and 9'-*cis*-ethyl 15,15'-dehydro- $\beta$ -apo-8'-carotenoate(C<sub>30</sub>) (in CDCl<sub>3</sub>).

Table 7. Chemical shifts (ppm) of the aldehydic proton of  $\alpha$ -methyl substituted conjugated aldehydes<sup>a</sup>

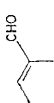
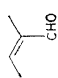
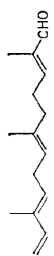
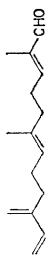


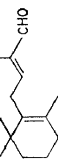
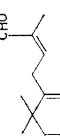
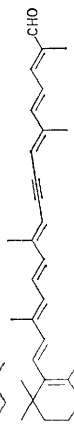
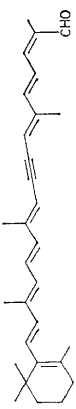

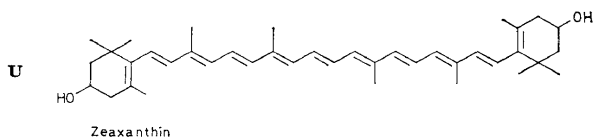
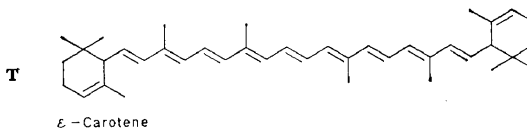
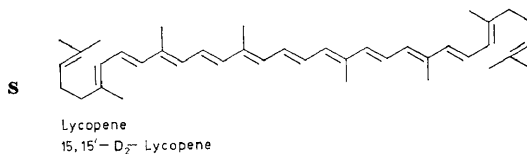
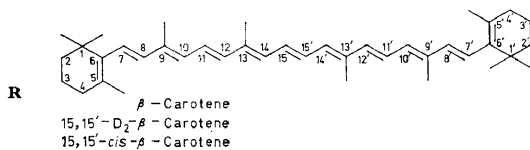
Compound	Chemical Structure	Trans (ppm)	Cis (ppm)
Tiglaldehyde		9.32 (CCl <sub>4</sub> )	
Angel aldehyde			10.10
$\alpha$ -Sinensal		9.65 (CCl <sub>4</sub> ) 9.70 (CCl <sub>4</sub> )	
$\beta$ -Sinensal		9.33 (CCl <sub>4</sub> ) 9.33 (CDCl <sub>3</sub> )	
2- <i>trans</i> -2,6-dimethyl-octa-2,6-dien-1-al		9.26 (CCl <sub>4</sub> )	
2- <i>cis</i> -2,6-dimethyl-octa-2,6-dien-1-al			10.01 (CCl <sub>4</sub> )
<i>trans</i> - $\beta$ -C <sub>14</sub> -aldehyde		9.32 (CCl <sub>4</sub> )	
<i>cis</i> - $\beta$ -C <sub>14</sub> -aldehyde			10.22 (CCl <sub>4</sub> )
9'- <i>trans</i> -15,15'-dehydro- $\beta$ -apo-8'-carotenal		9.47 (CDCl <sub>3</sub> )	
9'- <i>cis</i> -15,15'-dehydro- $\beta$ -apo-8'-carotenal			10.33 (CDCl <sub>3</sub> )
P 439 dialdehyde		9.46 (CDCl <sub>3</sub> )	

Table 8. Chemical shifts of proton magnetic

Compound	Olefinic hydrogens															
	2	2'	4	4'	6	6'	7	7'	8	8'	10	10'	11	11'	12	12'
R	—	—	—	—	—	—	~6·14		~6·14		6·14		6·65		6·34	
	—	—	—	—	—	—	~6·16		~6·16		6·16		6·65		6·36	
	—	—	—	—	—	—	~6·15		~6·15		6·15		6·67		6·41	
S																
	5·11	—	—		5·94		6·48		6·24		6·17		6·62		6·34	
	5·10	—	—		5·94		6·48		6·24		6·17		6·62		6·34	
T	—	—	5·40		2·17		5·51		6·10		6·11		6·60		6·33	
U	—	—	—	—	—	—	~6·11		~6·11		6·14		6·63		6·35	
V	—	—	—	—	—	—	6·21		6·34		6·27		6·63		6·41	
W	—	—	—	5·40	—	2·17	~6·14	5·52	~6·14	6·10	6·14	6·11	6·65	6·60	6·35	6·34
X	—	5·11	—	—	—	5·95	~6·15	6·49	~6·15	6·24	6·14	6·17	6·65	6·63	6·35	6·35
Y	—	5·10	5·40	—	2·17	5·94	5·51	6·48	6·09	6·24	6·10	6·17	6·60	6·62	6·32	6·34

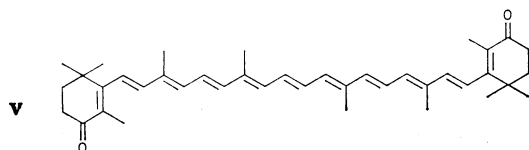
† assignment uncertain



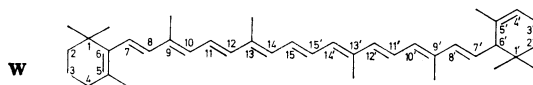
# PHYSICAL ORGANIC METHODS IN CAROTENOID RESEARCH

resonance signals (ppm) of carotenes (in  $\text{CDCl}_3$ ).

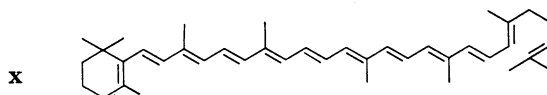
<i>Olefinic hydrogens (cont.)</i>				CH <sub>2</sub>								CH <sub>2</sub>					
14	14'	15	15'	1	1	5	5'	9	9'	13	13'	2	2'	3	3'	4	4'
6.24		~6.63		1.03		1.72		1.98		1.98		1.45		1.60		2.02	
6.26		—		1.03		1.71		1.97		1.97		1.46		1.59		~2.02	
~6.39		~6.65		1.02		1.73		1.98		1.98		1.46		1.60		2.01	
				1.63 ( <i>cis</i> ) 1.70 ( <i>trans</i> )		1.83		~1.97		~1.97							
~6.24		~6.62		1.62		1.83		~1.97		~1.97		—		~2.12		~2.12	
6.24		—		1.69								—		~2.11		~2.11	
~6.23		~6.62		0.82		1.58		1.91		1.95		~1.18		~2.00		—	
				0.90								~1.45					
6.24		~6.62		1.07		1.74		1.97		1.97		1.47		4.00		2.04	
												1.70				2.39	
~6.26		~6.65		1.19		1.87		1.99†		2.00†		1.85		2.51		—	
~6.24	~6.24	~6.62	~6.62	1.02	0.81	1.72	1.58	1.97	1.91	1.97	1.97	1.45	~1.18	~1.60	~2.00	~2.00	—
				0.90								~1.42					
~6.24	~6.24	~6.60	~6.60	1.03	1.61	1.72	1.83	1.97	1.97	1.97	1.97	1.45	—	~1.60	~2.11	2.02	~2.11
				1.69													
~6.24	~6.24	~6.60	~6.60	0.82	1.62	1.58	1.83	1.92	1.97	1.97	1.97	~1.19	—	~2.00	~2.11	—	~2.11
				0.90	1.69							~1.45					



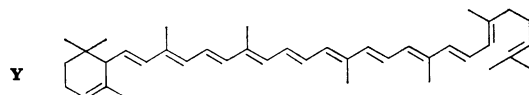
Canthaxanthin



$\alpha$ -Carotene



$\gamma$ -Carotene



$\delta$ -Carotene

than those of the corresponding *cis* isomers (10.0 to 10.3 ppm). The chemical shift of the aldehyde proton of P439 dialdehyde<sup>21</sup>, therefore, indicates the *trans* configuration of the chain<sup>22</sup>.

We have also included the carotenes in our studies. Table 8 summarizes some chemical shifts, measured in CDCl<sub>3</sub> solution. It is seen that all protons have been identified even in compounds with as much as 18 olefinic protons. Interestingly, the shifts of the olefinic protons of the unsymmetrical molecules can be obtained by taking the values from the two corresponding symmetrical compounds. The same method has previously been used for the assignment of the methyl protons<sup>19</sup>.

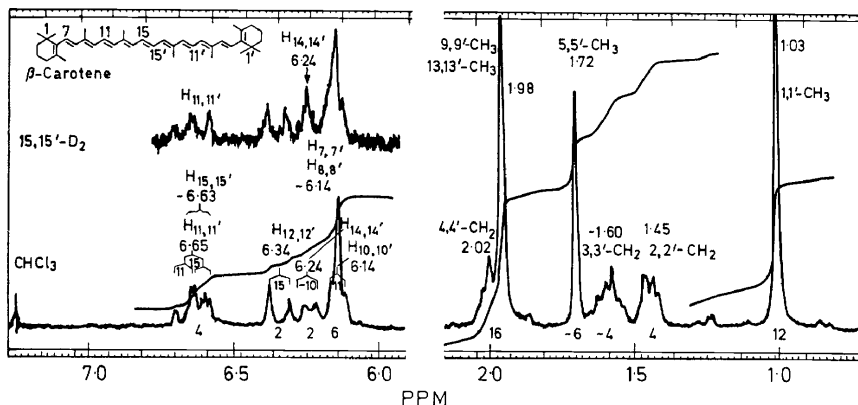


Figure 27. Proton magnetic resonance spectrum (220 MHz) of all-*trans*- $\beta$ -carotene (in CDCl<sub>3</sub>).

As an example Figure 27 shows the aliphatic and olefinic parts of the 220 MHz spectrum of  $\beta$ -carotene. Here the multiplets of the methylene protons in position 2 and 3 are clearly separated as has been found in all other compounds with  $\beta$ -end groups. In the olefinic range the assignment was again simplified by a comparison with the spectrum of 15,15'-D<sub>2</sub>- $\beta$ -carotene shown in the upper part of the spectrum.

Figure 28, our last example, presents the olefinic parts of the 220 MHz spectra of the symmetrical ( $\beta$ -,  $\epsilon$ - and lycopene) and the unsymmetrical carotenes ( $\alpha$ -,  $\delta$ - and  $\gamma$ -). A detailed comparison of the spectra of the latter with the spectra of the symmetrical compounds demonstrates the already mentioned additivity. Part of the assignments have actually been done by superimposing the experimental traces.

## MASS SPECTROMETRY

The development of proper sample introduction techniques has reduced the formerly difficult problem of the determination of the exact elemental composition of carotenoids to a routine task. With a high resolution mass spectrometer the molecular weight of a compound can be determined easily to within 5 ppm, which is sufficient for establishing the elemental composition unambiguously if only carbon, oxygen and hydrogen, the elements encountered in carotenoids up to now, are considered. By taking into account

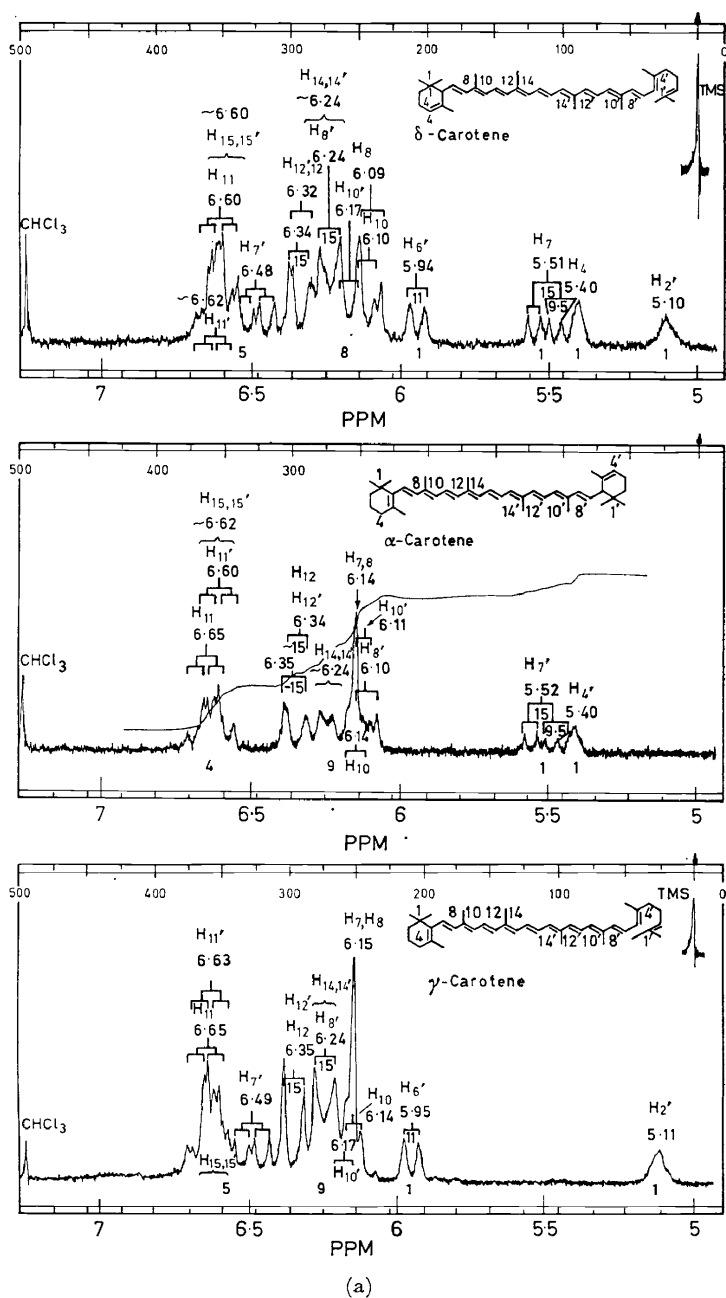
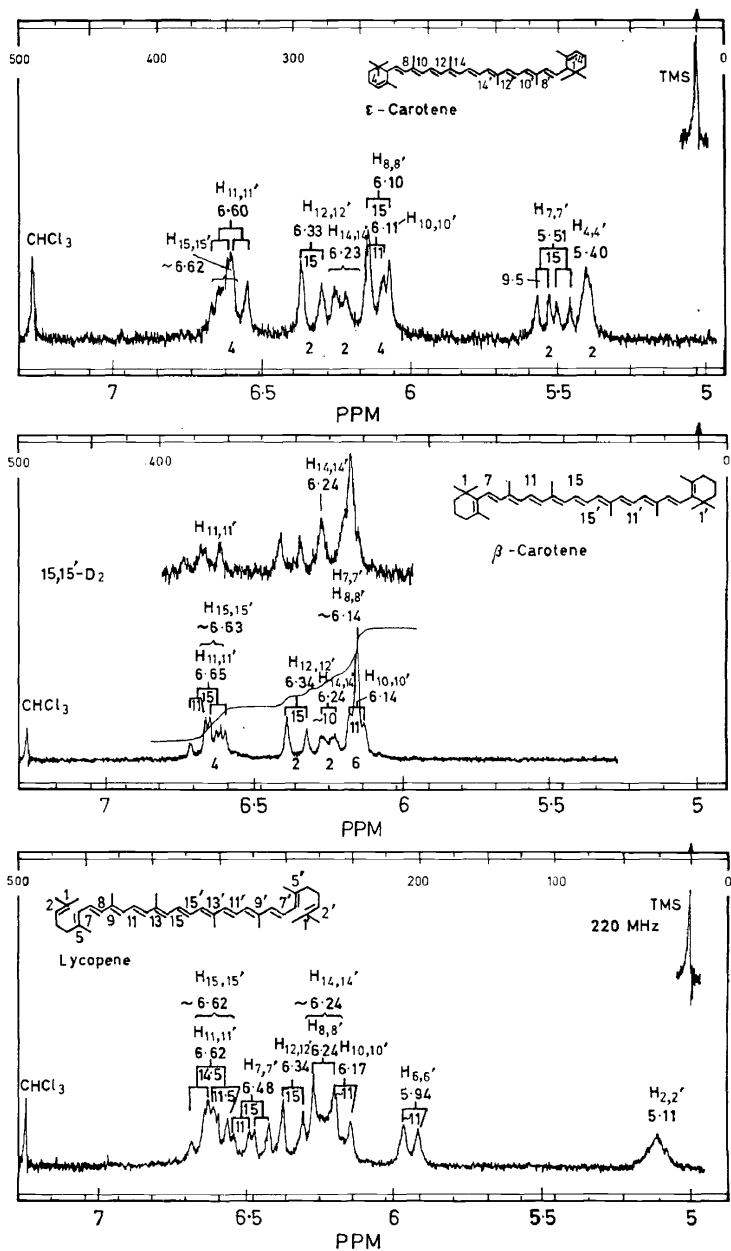


Figure 28. Olefinic region of the proton magnetic resonance spectra (220 MHz) of the carotenes (in  $\text{CDCl}_3$ ). [continued on page 404]





(b)

Figure 28. [continued from page 403]

the intensities and the precise masses of all the ions produced in major abundance, any other conceivable elemental composition could be established.

The mass spectra of unsubstituted carotenes exhibit fairly intense molecular ion peaks (*Figure 29*). At low ionizing voltage a major portion of the total ion current is carried by the molecular ions. The spectra of  $\beta$ -carotene, taken at

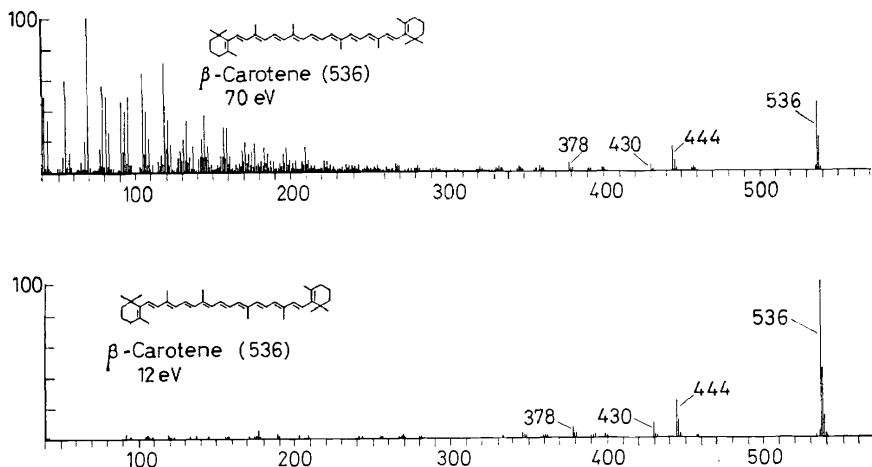


Figure 29. Mass spectra of  $\beta$ -carotene at 70 and 12 eV.

70 eV and about 12 eV, are typical examples for the general appearance of mass spectra of carotenoids. In substituted carotenoids, however, the molecular ion peak may be very small, due to a facile fragmentation involving a substituent, as is the case with the acetoxy group of fucoxanthin, or non-existent. Generally, two causes for the absence of molecular ions must be considered. One is a thermal decomposition of the sample during evaporation and the other is the fragmentation after electron impact. The second type of degradation appears to be less important in carotenoids than in most other classes of compounds, presumably due to the extended olefinic system, which confers some stability to the molecular ions. Thermal decomposition, however, is more of a problem with carotenoids than with many other types of compounds, due to the relatively high temperature needed to achieve sufficient vapour pressure for a spectrum. Carotenes are known to be thermally unstable compounds<sup>23</sup>. They cannot be sublimed in quantity without considerable decomposition. Care must therefore be taken, when running their mass spectra, to keep the temperature as low and the heating time as short as possible. All the spectra discussed below were obtained from samples which were placed on the tip of a ceramic rod within a quartz tube, next to the ion chamber of an MS 9 mass spectrometer. The distance of the sample from the electron beam was about 15 mm. The temperature of the ion chamber was kept constantly at 250° and the sample was evaporated by independently heating the quartz tube in order to achieve an adequate

vapour pressure in the chamber. Unfortunately, the temperature of the heated sample could not be measured. It is estimated to have been in the neighbourhood of 200° for  $\beta$ -carotene. In all cases about the same vapour pressure was generated to run the spectra. The time required from the beginning of the heating of the sample to the completion of the spectrum was normally 2 to 5 minutes. This procedure of sample introduction was chosen primarily to allow fast heating of the sample, but also to keep the conditions as uniform as possible for all the samples. Despite these precautions the spectra are much less reproducible than those of thermally more stable compounds. Spectra taken from carotene samples introduced in different ways or obtained from different mass spectrometers can only be compared in a qualitative manner. This is due to the fact that thermal decomposition cannot be totally avoided when a sample is introduced.

Although molecular weight and elemental composition are undoubtedly the most useful information which may be gained from a mass spectrum, the cracking pattern frequently reveals important details of the *structure*. In addition, the fragmentation of molecules in a mass spectrometer is sometimes an interesting topic for research.

The large conjugated system of double bonds does not prevent the carotene molecules from extensive fragmentation, when bombarded with 70 eV electrons. The spectrum of  $\beta$ -carotene (*Figure 29*) shows that by far the largest portion of the total ion current is spread among ions below  $m/e$  200. There is a peak at virtually every mass number, the more intense peaks always being at uneven mass numbers (representing even electron fragments) as is usual in unsaturated hydrocarbons. If the origin of such a peak is scrutinized by a search for its metastable precursors, then usually several such precursors are detected, indicating that these ions are formed by a number of multistep processes. Thus, there is little hope for extracting any structural information pertaining to the original molecules from these ions.

In order to investigate the possibility of distinguishing *cis-trans* isomers by mass spectrometry, the spectrum of 15,15'-*cis*- $\beta$ -carotene was run. It was indistinguishable from that of  $\beta$ -carotene, as expected from the experience gained with other *cis-trans* isomers.

Among the many unspecific fragments in the low mass range, there may be a few remarkable ones, if certain structural features are present in a molecule (*Figure 30*). In the spectrum of lycopene, for example, very intense peaks appear at  $m/e$  69 and 41. From a comparison of the intensities of these peaks, with those of the peaks at  $m/e$  69 and 41 in other carotenes without the  $\gamma$ -end group, e.g.  $\beta$ -carotene, it is evident, that they must be due to the terminal isopentenyl group. The ion at  $m/e$  69 originates from a simple cleavage of the doubly allylic bond and  $m/e$  41 represents a secondary fragmentation product of the ion 69.

In carotenoids which contain substituted end groups, intense peaks appear in the low mass region if a stable cation can be formed in a simple cleavage.

The peaks at  $m/e$  92 and  $m/e$  106 which appear in the spectra of carotenes correspond to molecular ions of toluene and xylene, respectively. A seven membered ring structure has been proposed for these ions<sup>24</sup>. Since the intensities of these peaks tend to vary considerably during the time a sample is being heated in the ion source, it is likely that they are due, at least in

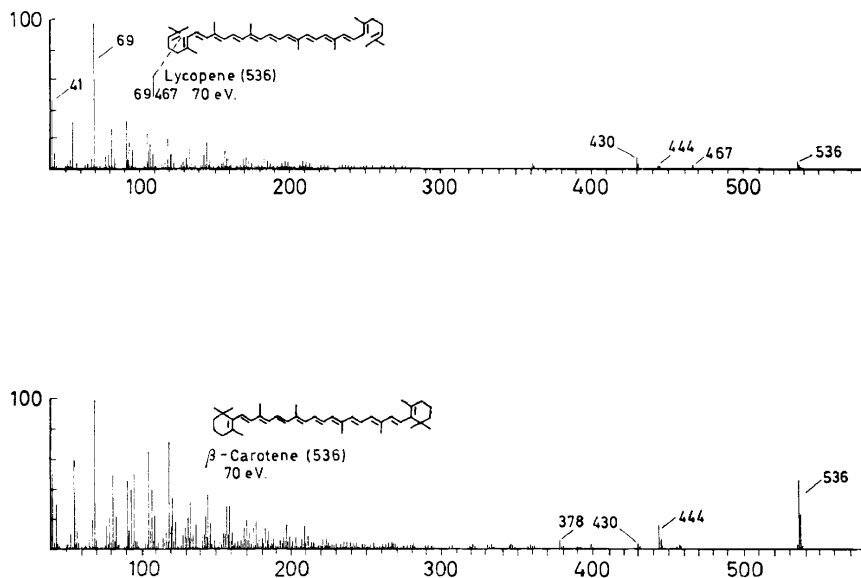


Figure 30. Formation of prominent low mass fragments from lycopene in comparison to  $\beta$ -carotene.

part, to the molecular ions of toluene and xylene formed by pyrolysis of the carotenes.

Much more revealing and interesting than the low mass region is the upper part of the mass spectra of carotenes, although the peaks are generally lower in number and in intensity. The ions appearing in the range above  $m/e$  300 may be divided into two classes, according to their origin. One portion represents the end groups while the other is formed from the polyene chain by expulsion reactions. A number of ions are formed by two consecutive reactions, usually one of each class<sup>19c</sup>.

## FRAGMENTATION OF THE END GROUPS

The fragmentation of the  $\alpha$ - and  $\gamma$ -end groups is sufficiently characteristic to permit the positive identification of one or both of these groups in a carotene or a carotenoid, at least as long as no functional group interferes with the fragmentation (Figure 30).

The presence of a  $\gamma$ -end group is indicated by a peak at  $M-69$ , which is directly derived from the molecular ion as indicated by an intense metastable peak. This ion is, of course, formed by cleavage of the same bond as the ion with mass 69, as discussed above, but with opposite charge distribution. The spectrum of a molecule with an  $\alpha$ -end group exhibits a peak for

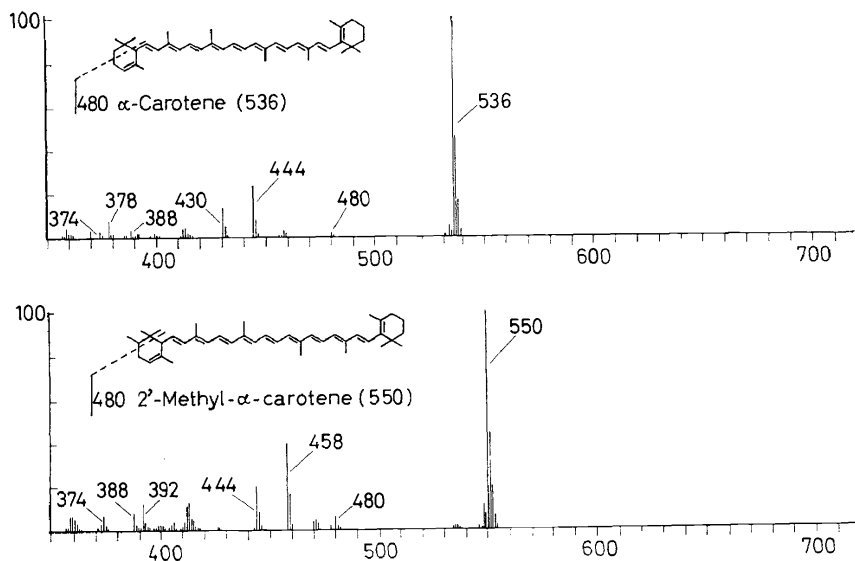


Figure 31. Typical fragmentation of  $\alpha$ -end groups A.

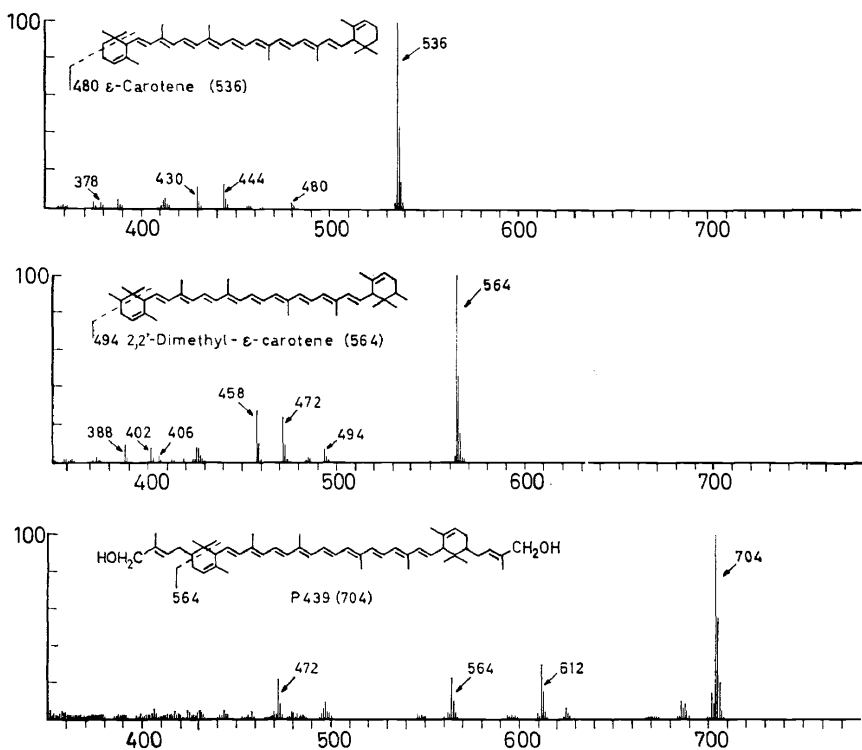


Figure 32. Typical fragmentation of  $\alpha$ -end groups B.

the loss of 56 mass units, due to a retro-Diels-Alder cleavage, first observed in  $\alpha$ -ionone<sup>25</sup> (Figure 31). Contrary to observations in other types of compounds containing cyclohexene rings, e.g. steroids, this reaction appears to be characteristic for this type of end groups. It is not observed in  $\beta$ -carotene, where it would lead to the loss of ethylene. The mass of the fragment arising from the retro-Diels-Alder reaction allows the localization of substituents in  $\alpha$ -end groups, as for example the methyl groups in 2'-methyl- $\alpha$ -carotene and in 2,2'-dimethyl- $\epsilon$ -carotene (Figures 31 and 32). A decisive argument for the structure of P 439, the first C<sub>50</sub>-carotenoid found in nature, was based on this fragmentation<sup>21</sup>. The  $\beta$ -end group does not undergo a specific fragmentation.

Other end groups containing functional groups have been reported to undergo characteristic fragmentation reactions. Carotenoid furanoid oxides for example show significant fragments<sup>24</sup>, which permit recognition of this type of compounds from their mass spectra. Ethyl apocarotenoids exhibit peaks due to loss of an ethoxy group<sup>26</sup>. On the other hand, some functional groups, e.g. aldehydes, do not give rise to very characteristic fragmentation<sup>26</sup>.

In general it may be stated that mass spectrometry frequently is a useful tool for the recognition of structural features at the chain ends of a carotene or a carotenoid. The pertinent peaks are, however, sometimes of low intensity and care has to be taken, when spectra of samples of less than perfect purity are to be interpreted.

## FRAGMENTATION OF THE END GROUPS OF THE POLYENE CHAIN

In the first paper<sup>19c</sup> dealing with the mass spectra of carotenes, peaks at mass numbers corresponding to the loss of 92 and 106 units from the molecular ions were attributed to ions formed by expulsion of toluene and xylene from the polyene chain. Subsequently it was observed that this type of fragmentation was common to all carotenoids and apocarotenoids which contain a chain of at least 8 conjugated double bonds. To a small extent, it occurs, however, also in molecules with a shorter polyene chain, so that no exact lower limit of the necessary chain length can be given.

The ratios of the abundances of the M-92 and M-106 ions differ considerably in the spectra of the various compounds investigated. From a study of a number of carotenoids, Enzell *et al.*<sup>28</sup> concluded that this ratio can be correlated qualitatively with the number of conjugated double bonds present in the acyclic portion of the polyene chain: lengthening of the chain causes a marked increase of the loss of xylene (M-106) at the expense of the loss of toluene (M-92).

Another observation made in connection with these fragmentations was that a relatively intense metastable peak appears for the loss of toluene, whereas none is present for the loss of xylene, even in those cases where this fragmentation is very prominent<sup>19c, 28</sup>. This fact has led to the suggestion, that two different mechanisms are operative in the two reactions<sup>28</sup>.

Another peak, M-158, corresponding to the loss of  $C_{12}H_{14}$ , has been attributed to an analogous reaction taking place in the polyene chain<sup>29</sup>.

Each of these fragmentations possesses its analogue in thermal degradation reactions, which have been observed in a number of carotenes and carotenoids. Kuhn und Winterstein established in 1932, that toluene and m-xylene were produced by thermal treatment of a variety of such compounds<sup>23</sup>. Shortly afterwards, 2,6-dimethylnaphthalene could be identified as one of the major degradation products by the same workers<sup>30</sup>. The relation between the M-92 and M-106 peaks in the mass spectrum and the formation of toluene and m-xylene on pyrolysis is self-evident. It is worth noting that in the case of bixin, the thermally generated product corresponding to the loss of xylene has been isolated and characterized<sup>31</sup>. The connection between the loss of  $C_{12}H_{14}$  in the mass spectrometer and the pyrolytic formation of dimethylnaphthalene, with the molecular formula  $C_{12}H_{12}$ , requires the assumption that the  $C_{12}H_{14}$ -unit is 1,6-dimethylcyclo-decapentaene, which under the conditions of the pyrolysis cyclizes with loss of  $H_2$  to form 2,6-dimethylnaphthalene. Since such reactions are well known to occur on pyrolysis, the relationship between these thermal and mass spectrometric degradation reactions also appears plausible.

These connections between mass spectrometric fragmentation and thermal behaviour of the carotenes appeared sufficiently interesting to investigate the matter in more detail.

To check the generality of the rule proposed by Enzell *et al.*, relating the chain length to the ratio of the intensities of the peaks at M-92 and M-106, the mass spectra of two isoprenologues of  $\beta$ -carotene, containing 50 and 60 carbon atoms, were investigated (*Figure 33*). The spectra clearly support the rule. In both compounds the intensity of the peak at M-106 significantly exceeds that at M-92. Due to their long polyene chains these compounds can undergo these expulsion reactions several consecutive times. According to the rule, the ratio of the loss of toluene to the loss of xylene should increase as the chain length decreases in the degradation. Two such steps can be discerned clearly in the  $C_{60}$ -case and again the experimental facts support the rule: the fragmentation is shifted in favour of the loss of toluene as the chain becomes shorter.

All carotenes investigated so far<sup>19c</sup> have contained the same distribution of methyl groups in their polyene chain. The differences in the intensity ratios of the ions M-92 and M-106, which occur in the spectra of molecules with *equal* numbers of double bonds in the acyclic portions of their chains, e.g.  $\alpha$ - and  $\beta$ -carotene, must therefore be explained by some steric or electronic effects of the end groups on the fragmentation of the chain. It appeared interesting to compare the mass spectra of two compounds which were identical with regard to chain length and end groups, but which had a different set of methyl groups in the chain. For this purpose a compound was synthesized in which the methyl group in position 13 was shifted to position 14, resulting in an 'unsymmetrical  $\beta$ -carotene' (*Figure 34*).

The spectrum of this compound, when compared with that of  $\beta$ -carotene, shows a remarkable change in the intensity ratio of the peaks M-92 and M-106. This result can best be explained by the assumption, that, in

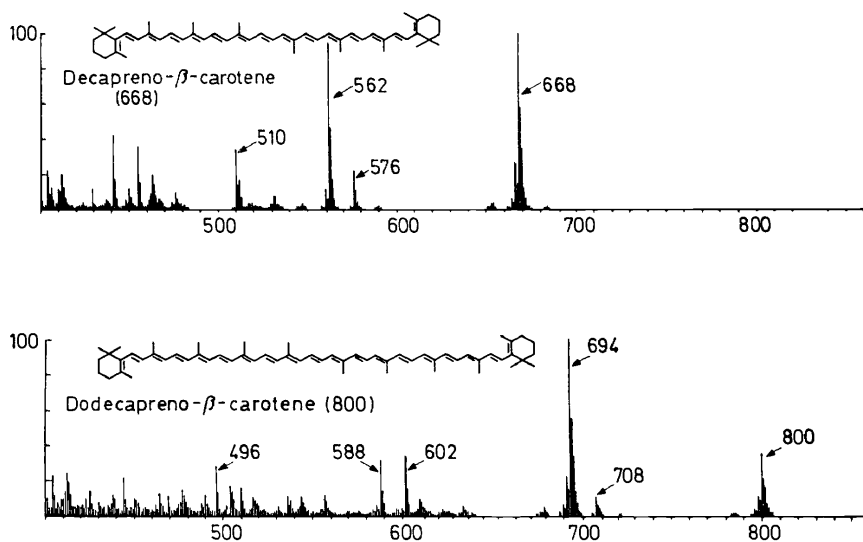


Figure 33. Mass spectra of decapreno- and dodecapreno- $\beta$ -carotene (70 eV).

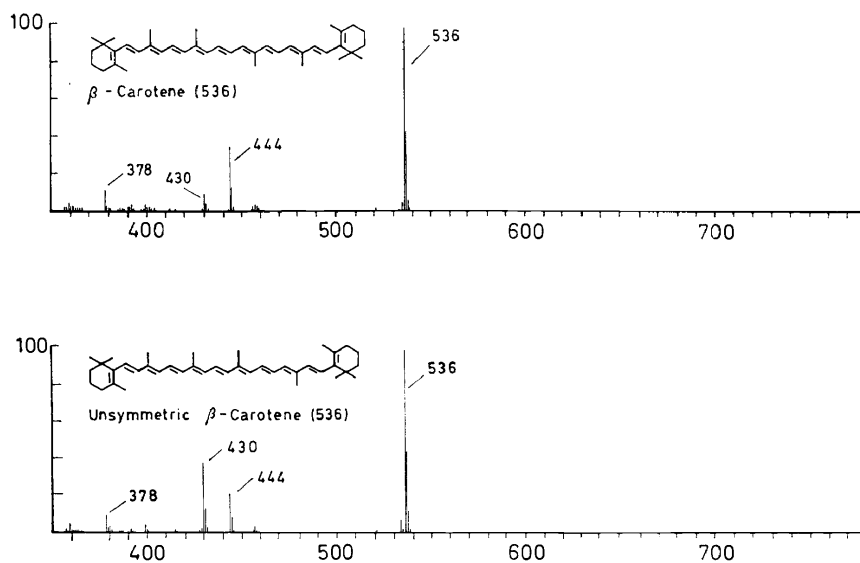


Figure 34. Mass spectrum of unsymmetrical  $\beta$ -carotene in comparison to  $\beta$ -carotene (70 eV).



$\beta$ -carotene, toluene is expelled mainly from the central portion of the chain. The shift of a methyl group towards the centre of the chain should then cause part of that central region, which normally is eliminated as toluene, to be lost as xylene. If this assumption is correct a metastable peak should be found for xylene in this case. Indeed, a small metastable peak was detected for this reaction.

The discovery of a metastable peak for the loss of xylene in this special case led to a careful search for metastable peaks in cases where they have been reported to be missing<sup>19c,28</sup>. This search appeared to be particularly important, in view of the previously mentioned suggestion<sup>28</sup> that different mechanisms should be considered for the formation of the ions M-92 and M-106. From the results discussed so far, it is possible that the difference between the two reaction mechanisms consists in the fact that one is a thermal degradation (not exhibiting a metastable peak) and the other an electron impact induced fragmentation. The loss of xylene in the unsymmetrical  $\beta$ -carotene would then have to be considered of mixed nature. In the search for metastable peaks the very sensitive method of Barber and Elliott<sup>32</sup> was employed. As a result of these experiments, metastable peaks could be detected for all reactions in question (*Figure 35*). The metastable spectra for the peaks at M-92, M-106 and M-158 of  $\beta$ -carotene serve as an example for these measurements. While in this case all the metastable peaks found were of relatively high intensity, as compared to the corresponding peaks for the ions formed in the ion source, cases were encountered where these peaks were very small. The most prominent example of this type of results was the peak at M-106 in lycopene. The intensity of the corresponding metastable peak amounted to only 0.2 per cent of the normal peak, as compared to the 5 to 20 per cent values encountered in  $\beta$ -carotene. Although these experiments proved beyond question that the observed ions were, at least in part, formed *after* ionisation of the molecules, they did not exclude contributions of thermally formed species to the peaks. It therefore became essential to prove that the possibility of the thermal origin of the peaks did indeed exist under the conditions employed.

A sample of lycopene was introduced into the mass spectrometer and the ratios of M-92/M and M-106/M were plotted against time (*Figure 36*). The results obtained were somewhat surprising. The peaks suspected to be partially due to pyrolysis first gained intensity as compared to the molecular ion, as was to be expected. After a few minutes, however, the ratio changed gradually in favour of the molecular ion, being lower at the end of the experiment than at the beginning. To explain these results, it has to be assumed that two competitive thermal reactions are taking place, while the sample is heated. One type of reaction causes the lycopene to lose toluene and xylene, thus forming M-92 and M-106 molecules. At the same time part of the lycopene isomerizes in such a way, that it is no longer able to lose toluene and xylene. Thus, at the beginning of the experiment the amounts of M-92 and M-106 are growing. When their production stops after a few minutes, due to the fact that all the remaining lycopene has isomerized into its stable form, the curve starts to decline as the evaporation of the lower boiling M-92 and M-106 species continues after their formation has ceased.

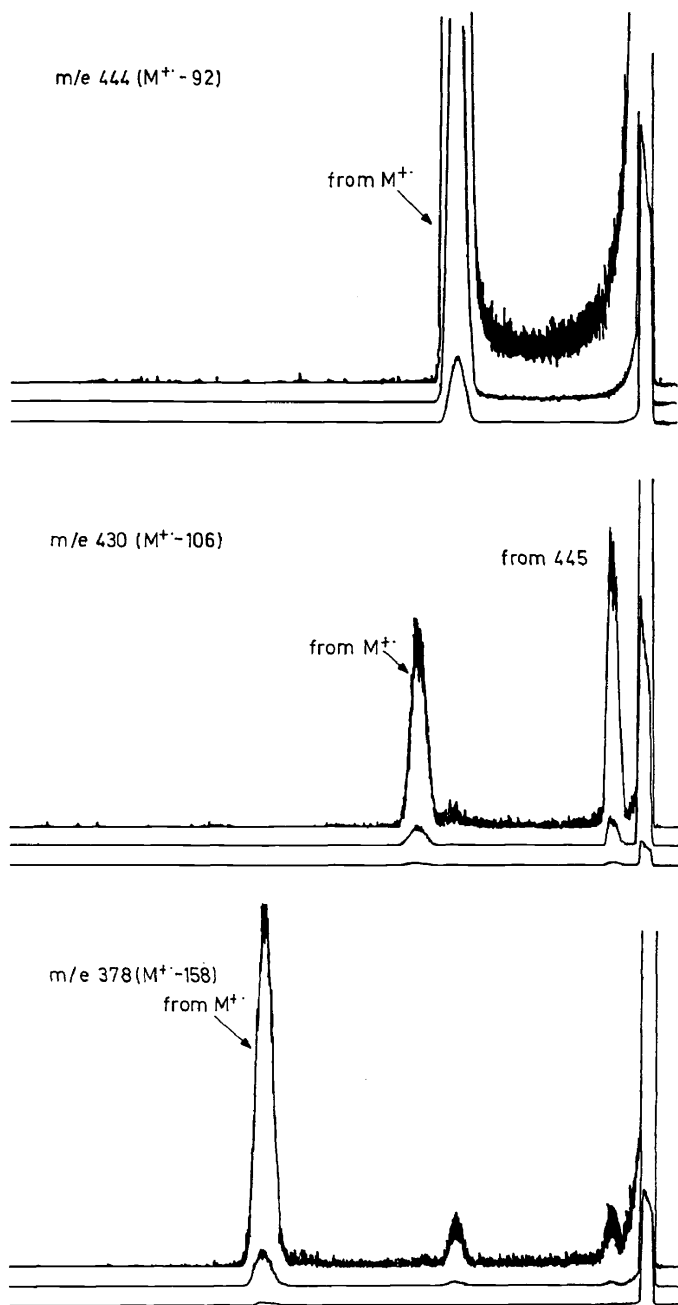


Figure 35. Peaks  $m/e\ 444\ (M-92)$ ,  $m/e\ 430\ (M-106)$  and  $m/e\ 378\ (M-158)$  formed from metastable molecular ions of  $\beta$ -carotene.

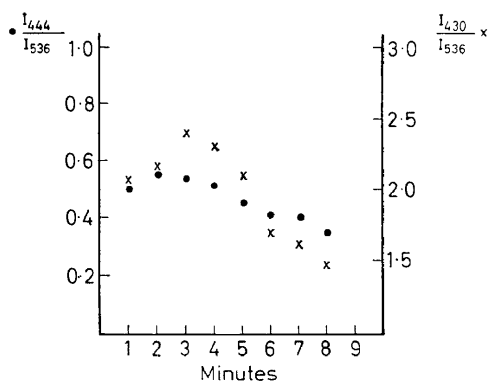


Figure 36. Variation of intensity ratios  $m/e$  430/536 and  $m/e$  444/536 with time in the mass spectrum of lycopene (12 eV).

In order to gain further insight into this problem, lycopene and  $\beta$ -carotene were subjected to pyrolytic degradation prior to mass spectrometric investigation of the samples. Small portions of these compounds were heated to  $250^\circ$  for 10 minutes under  $\text{CO}_2$ . This treatment was sufficient to convert the crystalline powders into pale yellow liquids, whose UV spectrum indicated that no carotenes were left. Samples of these oils were then introduced into the mass spectrometer in such a manner that fractions of different volatility could be observed separately.  $\beta$ -Carotene and lycopene showed essentially the same behaviour. Toluene, xylene and dimethylnaphthalene appeared first. On heating the samples, these compounds disappeared and the spectra of the higher boiling fractions could be observed, as is illustrated for lycopene (Figure 37). Clearly a molecule ( $M:430$ ) corresponding to the loss of xylene had been formed. The fragmentation of this compound ( $m/e$  341 corresponding to the loss of the isopentenyl radical) indicates that it has retained at least one of the original end groups. On further heating, the pattern changed and a spectrum appeared which showed most of the characteristics of the spectrum of lycopene; i.e. the molecular ion at  $m/e$  536 and a peak at  $M-69$ . However, only small peaks due to loss of 92 and 106 mass units are present. This spectrum therefore lends support to the hypothesis that lycopene isomerizes partially to a more stable compound on heating. Later, peaks appear at higher mass numbers indicating polymerisation.

From these data it must be concluded that mass spectra obtained from carotenes and related compounds have to be considered as due to mixtures of the original samples with more or less considerable amounts of thermally degraded and isomerized material, depending on the experimental conditions of the introduction of the samples. Accordingly, the poor reproducibility of these spectra is easily understood.

In view of the intricate relationship between these thermal and electron impact induced reactions, we attempted to learn something about their mechanisms. For this purpose  $15,15'\text{-D}_2\text{-}\beta$ -carotene and  $15,15'\text{-D}_2$ -lycopene were synthesized. In Figure 38 the mass spectrum of the deuterated  $\beta$ -



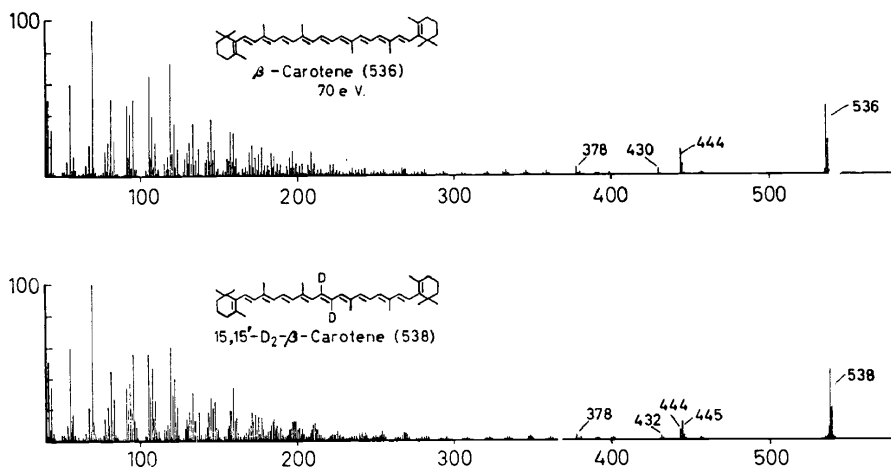


Figure 38. Mass spectrum of 15,15'-D<sub>2</sub>- $\beta$ -carotene in comparison to  $\beta$ -carotene (70 eV).

carotene is shown in comparison with  $\beta$ -carotene. Qualitatively it is easily seen that mono- and dideuterated toluene are lost in about equal amounts, leading to the peaks at  $m/e$  444 and 445. Xylene is lost essentially without deuterium whereas the dimethylcyclodecapentaene contains both deuterium atoms. With lycopene, essentially the same results are obtained, except that part of the toluene is lost without deuterium.

The most significant conclusions to be drawn from these results are that scattering of deuterium does not occur in these compounds to an appreciable extent and that the reactions indeed take place in well defined portions of the chain. The problem then was to find a mechanism by which all the various facts could be accounted for.

A mechanism for the thermal loss of toluene and xylene involving a 4-membered ring intermediate, has been proposed by Edmunds and Johnstone<sup>33</sup> (Figure 39). Although this mechanism is not the only one which can be written for these reactions, it rationalizes all the essential results of the thermal as well as the electron impact induced fragmentation of the carotenes.

If the loss of toluene, xylene and C<sub>12</sub>H<sub>14</sub> from 15,15'-D<sub>2</sub>- $\beta$ -carotene is considered in the light of this mechanism, a scheme is obtained, from which all the possible ways for forming the products in question can be deduced (Figure 40). The validity of the mechanism can be judged by qualitative comparison of the predictions with the experimental results.

The mechanism requires the loss of xylene without deuterium, which is in agreement with the experiment. Toluene, on the other hand, can only be expelled with one or two deuterium atoms, as is observed. Dimethylcyclodecapentaene can only be lost with both deuterium atoms, again as found. Thus, there is excellent agreement between the predictions made and the results of the mass spectrometric experiments.

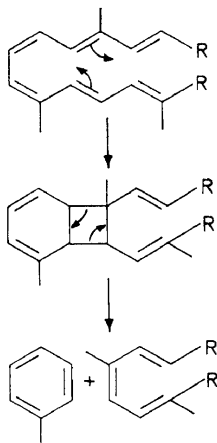


Figure 39. Mechanism for the formation of aromatic compounds from polyenes<sup>33</sup>.

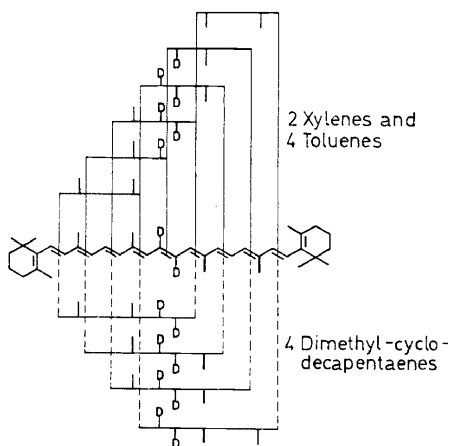


Figure 40. Possibilities for the loss of toluene, xylene and dimethylcyclodecapentaenes from 15,15'-D<sub>2</sub>-β-carotene.

In order to determine whether the mechanism is in agreement also with the results of thermal reactions, deuterated β-carotene was pyrolyzed as described before and the low boiling fractions were examined in the mass spectrometer (Figure 41). Besides ionene,<sup>34</sup> which is a pyrolysis product known to be formed from the end groups of β-carotene, toluene, xylene and dimethylnaphthalene are observed. In the spectrum of the deuterated compound the results are in perfect agreement with the mechanism. Toluene contains one and two deuterium atoms, xylene practically none. Most interesting is the case of dimethylnaphthalene, which contains only one

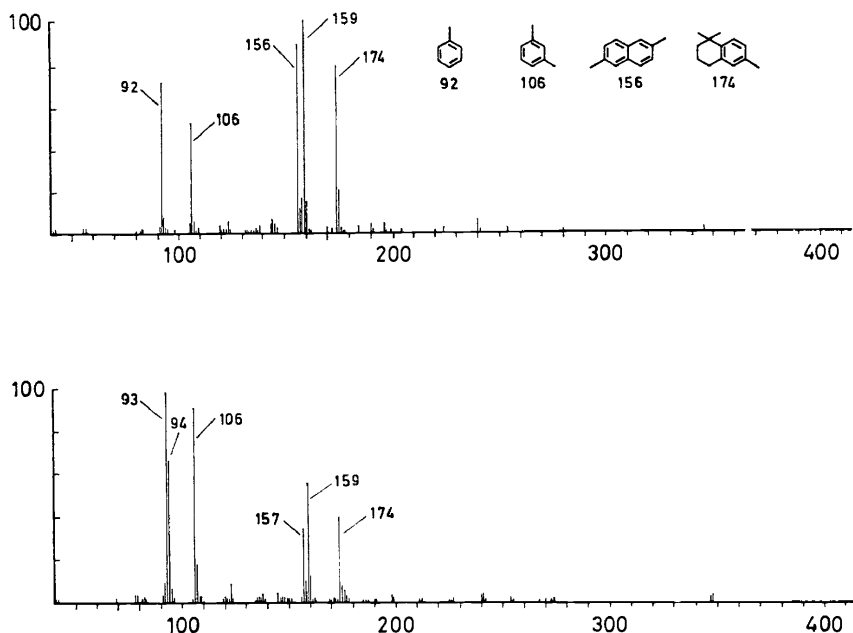


Figure 41. Mass spectra (12 eV) of the low boiling fraction of thermally pretreated samples (10 minutes at 250°) of  $\beta$ -carotene and 15,15'- $\beta$ -carotene.

deuterium, although the corresponding dimethylcyclodecapentaene has to contain two deuterium atoms. From the work of Kuhn and Winterstein, it is known that the methyl groups are exclusively in positions 2 and 6 of the naphthalene. The corresponding precursor, 1,6-dimethylcyclodecapentaene is one of the two possibilities allowed by the mechanism. Perhaps for steric reasons the other possible product containing the methyl groups in positions 1 and 5 is apparently not formed. The conversion of the 1,6-dimethylcyclodecapentaene could lead to either 1,5- or 2,6-dimethylnaphthalene via electrocyclic ring closure and aromatisation by dehydrogenation. Again probably for steric reasons only one, the 2,6-product is formed. Given these facts, only the loss of DH from the 3,4-D<sub>2</sub>-1,6-dimethylcyclodecapentaene can lead to 2,6-dimethylnaphthalene, which thus can only contain one deuterium as is indeed observed.

All these results are summarized in Table 9. The experimentally found percentages are only approximate, due to the uncertainties of the measurements of isotopic abundancies in mixtures and in thermally labile samples. Nevertheless the figures appear in such good agreement with the predictions of the mechanism, that the latter should be adopted to explain the mass spectrometric fragmentations of the polyene chains.

Table 9. Deuterium distribution calculated (possibilities) and found for the thermal degradation and the corresponding mass spectrometric fragmentation products of 15,15'-D<sub>2</sub>-β-carotene.

			D <sub>0</sub>	D <sub>1</sub>	D <sub>2</sub>
Toluene	found:	possibilities	0	50	50
		mass spectrum†	0	60	40
		thermal	0	60	40
Xylene	found:	possibilities	100	0	0
		mass spectrum†	>90	<10	
		thermal	90	10	
Dimethylcyclodecapentaene	found:	possibilities	0	0	100
		mass spectrum†	<20		>80
		thermal	→ Dimethylnaphthalene		
Dimethylnaphthalene	found:	possibilities	0	100	0
		thermal	10	80	10

† = calculated from the M--toluene, M--xylene and M--dimethylcyclodecapentaene peak.

We wish to thank Prof. Dr. H.-J. Cantow, University of Freiburg i. Br., for permission to use the Varian 220 MHz p.m.r. spectrometer and Dr. J. Würsh and co-workers (F. Hoffmann-La Roche & Co. Ltd., Basle) for the preparation of the labelled compounds.

## References

- 1 A. Wasserman. *J. Chem. Soc.* 979 (1959).
- 2 P. E. Blatz and D. L. Pippert. *J. Am. Chem. Soc.* **90**, 1296 (1968).
- 3 A. Wasserman. *Mol. Phys.* **2**, 226 (1959).
- 4 T. S. Sorensen. *J. Am. Chem. Soc.* **87**, 5075 (1965).
- 5 O. Isler and P. Schudel. *Advances in Organic Chemistry, Methods and Results* (Eds. R. A. Raphael, E. C. Taylor and H. Wynberg) Vol. IV, p. 115, Interscience Publishers, New York (1963).
- 6 J. H. C. Smith. *J. Am. Chem. Soc.* **58**, 247 (1936).
- 7 L. Zechmeister and A. Polgar. *J. Am. Chem. Soc.* **65**, 1522 (1943).
- 8 K. Hirayama. *J. Am. Chem. Soc.* **77**, 373 (1955).
- 9 J. Dale. *Acta Chem. Scand.* **8**, 1235 (1954); **11**, 265 (1957).
- 10 B. C. L. Weedon. *Chem. in Britain* **3**, 424 (1967).
- 11 S. L. Jensen. *Pure Appl. Chem.* **14**, 227 (1966).
- 12 K. Lunde and L. Zechmeister. *J. Am. Chem. Soc.* **77**, 1647 (1955).
- 13 E. Nocoară, V. Tămaş, G. Neamtu and C. Bodea. *Liebigs Ann.* **697**, 201 (1966).
- 14 H. Mayer. [F. Hoffmann-La Roche, Basle (Switzerland)], unpublished results.
- 14a *trans*-β-Ionylidene crotonic acid  
E. L. Eichhorn and C. H. MacGillavry. *Acta Cryst.* **12**, 872 (1959).
- 14b *cis*-β-Ionylidene crotonic acid  
B. Koch and C. H. MacGillavry. *Acta Cryst.* **16**, A48 (1963).
- 14c *Vitamin A acid* (all-*trans*, triclinic modification)  
C. H. Stam and C. H. MacGillavry. *Acta Cryst.* **16**, 62 (1963).
- 14d 7,7'-Dihydro-β-carotene  
C. Sterling. *Acta Cryst.* **17**, 500 (1964).
- 14e β-Carotene  
C. Sterling. *Acta Cryst.* **17**, 1224 (1964).
- 14f 15,15'-Dehydro-β-carotene  
W. G. Sly. *Acta Cryst.* **17**, 501 (1964).
- 14g *Canthaxanthin*  
J. C. J. Bart and C. H. MacGillavry. *Acta Cryst.* **24**, 1587 (1968).
- 14h 15,15'-Dehydrocanthaxanthin  
J. C. J. Bart and C. H. MacGillavry. *Acta Cryst.* **24**, 1569 (1968).



- 15 G. A. Coulson. *J. Chem. Phys.* **7**, 1069 (1939).
- 16 L. Pauling. *Fortschr. Chem. Org. Naturstoffe* **3**, 203 (1939).
- 17 M. Buchwald and W. P. Jencks. *Biochemistry* **7**, 834 (1968).
- 18 M. S. Barber, J. B. Davis, L. M. Jackman and B. C. L. Weedon. *J. Chem. Soc.* 2870 (1960).
- 19a B. C. L. Weedon. *Chemistry and Biochemistry of Plant Pigments*, (Ed. T. W. Goodwin), p. 75, Academic Press, London, (1965).
- 19b S. L. Jensen and A. Jensen. *Progr. Chem. Fats and Lipids*, (Ed. R. T. Holman), Vol. VIII, part 2, p. 129, Pergamon Press, Oxford (1965).
- 19c U. Schwieter, H. R. Bolliger, L. H. Chopard-dit-Jean, G. Englert, M. Kofler, A. König, C. v. Planta, R. Ruegg, W. Vetter and O. Isler. *Chimia (Switz.)* **19**, 294 (1965).
- 20 D. J. Patel, *Nature* **221**, 825 (1969).
- 21 S. L. Jensen, S. Hertzberg, O. B. Weeks and U. Schwieter. *Acta Chem. Scand.* **22**, 1171 (1968).
- 22 U. Schwieter and S. L. Jensen. *Acta Chem. Scand.*, **23**, 1057 (1969).
- 23 R. Kuhn and A. Winterstein. *Chem. Ber.* **65**, 1873 (1932).
- 24 R. Bonnet, A. K. Mallams, A. A. Spark, J. L. Tee, B. C. L. Weedon and A. McCormick. *J. Chem. Soc.* 429 (1969).
- 25 K. Biemann. *Mass Spectrometry*. McGraw Hill, New York, p. 103 (1962).
- 26 U. Schwieter, H. Gutmann, H. Lindlar, R. Marbet, N. Rigassi, R. Ruegg, S. F. Schaeren and O. Isler. *Helv. Chim. Acta* **49**, 369 (1966).
- 27 J. Baldas, Q. N. Porter, L. Cholnoky, J. Szabolcs and B. C. L. Weedon. *Chem. Comm.* 852 (1966).
- 28 C. R. Enzell, G. W. Francis and S. L. Jensen. *Acta Chem. Scand.* **22**, 1054 (1968).
- 29 C. R. Enzell, G. W. Francis and S. L. Jensen. *Acta Chem. Scand.*, **23**, 727 (1969).
- 30 R. Kuhn and A. Winterstein. *Chem. Ber.* **66**, 429, 1733 (1933).
- 31 G. G. McKeown, *Journal of the A.O.A.C.* **48**, 835 (1965).
- 32 M. Barber and R. M. Elliott. *Proceedings of the 12th. ASTM Conference*, Montreal, (1964).
- 33 F. S. Edmunds and R. A. W. Johnstone. *J. Chem. Soc.* 2892 (1965).
- 34 W. C. Day and J. G. Erdman. *Science* **141**, 808 (1963).